

# GREEN AMMONIA PRODUCTION

## ELECTRIFIED HABER-BOSCH PROCESS



### Group members:

Yara Hamade	4982754
Kevin Tran	4904672
Cas Visschers	4912705

**Course:** WB3595 Design Project  
Renewables Based Energy Conversion and  
Storage

**Supervisor:** Prof. Dr. Ir. Wiebren de Jong

**Supervisor:** Dr. Ir. Mahinder Ramdin

Date: 14-1-2022  
Study year: 2021-2022  
Group number: 12



Delft University of Technology



# ABSTRACT

This report provides a design for a new process to make the ammonia-producing Haber-Bosch process more sustainable by reducing its CO<sub>2</sub> emissions. It presents different elements of a process design with most importantly; process diagrams, mass and energy balances and a techno-economic analysis. The most important differences in this process is the use of water electrolysis and nitrogen production. This process emits approximately 50 % less CO<sub>2</sub> than regular Haber-Bosch methods. Nevertheless, the techno-economic analysis shows that this method is very expensive and that ammonia can only be sold at an acceptable price conform to the market with subsidies on electricity prices and can only become competitive if CO<sub>2</sub> taxes are implemented for classic Haber-Bosch plants.



# TABLE OF CONTENTS

<b>Introduction</b>	<b>ix</b>
<b>1 Literature Summary</b>	<b>1</b>
1.1 Green Electrons Process . . . . .	1
1.2 SMR Based Hydrogen Production . . . . .	1
1.3 Nuclear Based Hydrogen Production . . . . .	1
1.4 Biomass Based Hydrogen Production . . . . .	2
1.5 Electrolysis Based Hydrogen Production . . . . .	3
1.6 Nitrogen Purification . . . . .	3
1.7 Electrified Haber-Bosch Process . . . . .	4
1.8 Feasibility . . . . .	4
1.9 Conclusion . . . . .	4
<b>2 Conceptual Process Design</b>	<b>5</b>
2.1 Process Creation . . . . .	5
2.1.1 Batch vs. Continuous Process . . . . .	5
2.1.2 Raw Materials and Products Specification . . . . .	6
2.1.3 Process Synthesis . . . . .	6
2.2 Process Design . . . . .	7
2.2.1 Functions Diagram . . . . .	7
2.2.2 Hydrogen and Nitrogen storage for steady state operation . . . . .	8
2.2.3 Units of Operation and Detailed Preliminary Design . . . . .	9
2.3 Energy source of the plant . . . . .	12
<b>3 Mass and Energy Balances</b>	<b>15</b>
3.1 Mass balances . . . . .	15
3.1.1 Ammonia synthesis . . . . .	15
3.1.2 Hydrogen electrolysis . . . . .	15
3.2 Energy balances . . . . .	16
3.2.1 Ammonia synthesis . . . . .	16
3.2.2 Hydrogen electrolysis . . . . .	18
3.3 Sizing and Scaling . . . . .	19
3.4 Detailed Estimate Design Based on Mass and Energy Balances . . . . .	19
<b>4 Techno-economic Analysis</b>	<b>23</b>
4.1 Electricity prices . . . . .	23
4.2 Capital Costs . . . . .	24
4.2.1 Electrolyser costing . . . . .	24
4.2.2 Compressor costing . . . . .	25
4.2.3 Heat exchanger costing . . . . .	25

4.2.4	Reactor costing	25
4.2.5	Cooling tower costing	26
4.2.6	Electric furnace costing	26
4.2.7	Flash separator costing	26
4.2.8	Nitrogen storage costing	26
4.2.9	Total CAPEX	27
4.3	Operational Costs	28
4.3.1	Operating Labour	28
4.3.2	Summary of operational costs	28
4.4	NPV Calculation	29
4.5	Levelized Cost of Ammonia	30
<b>5</b>	<b>Comparison of CO<sub>2</sub> Emissions</b>	<b>31</b>
5.1	CO <sub>2</sub> intensity	31
5.2	Comparison conventional Haber-Bosch Process	31
5.2.1	hydrogen production	31
5.2.2	regeneration	32
5.2.3	ammonia production	32
<b>6</b>	<b>Discussion</b>	<b>33</b>
<b>7</b>	<b>Conclusion</b>	<b>35</b>
<b>8</b>	<b>Bibliography</b>	<b>37</b>
<b>A</b>	<b>Multi criteria analysis</b>	<b>43</b>
A.1	hydrogen electrolysis	43
A.1.1	Performance criteria	43
A.1.2	weightings	43
A.1.3	Concepts	44
A.1.4	multi criteria analysis	44
A.2	nitrogen purification	45
A.2.1	Performance criteria	45
A.2.2	weightings	45
A.2.3	Concepts	45
A.2.4	Criteria analysis	45
<b>B</b>	<b>Aspen model</b>	<b>47</b>
<b>C</b>	<b>Python scripts hydrogen electrolysis</b>	<b>49</b>
C.1	mass balance	49
C.2	energy balance	50
<b>D</b>	<b>Energy consumption</b>	<b>53</b>
D.1	ammonia synthesis	53
D.1.1	compressors	53
D.1.2	heaters	53

---

D.2	hydrogen electrolysis . . . . .	54
D.3	nitrogen purification . . . . .	54
D.4	cooling and regeneration . . . . .	54
D.5	Total . . . . .	54
D.6	wind farm for case two . . . . .	54
<b>E</b>	<b>Sizing &amp; scaling</b>	<b>55</b>
E.1	Reactor sizing . . . . .	55
E.2	Flash separator sizing . . . . .	56
E.3	Nitrogen pressure vessel . . . . .	57
E.4	Hydrogen storage vessel . . . . .	58
<b>F</b>	<b>Techno-economic analysis</b>	<b>59</b>
<b>G</b>	<b>Cooling</b>	<b>63</b>
G.1	power cycle . . . . .	63
G.2	Reactor cooling . . . . .	65
G.3	Economic feasibility . . . . .	65



# INTRODUCTION

Ammonia is one of the most highly produced chemicals in the world today and the agricultural sector heavily relies on its production. In fact, 80 % of the ammonia produced in the world goes to the production of fertilizers. It is mainly produced by the Haber-Bosch process, which converts  $N_2$  to  $NH_3$  by a reaction with  $H_2$ . Unfortunately, this process is very energy intensive as the conversion is conducted at pressures above 300 bar and temperatures between 400 and 500 °C. It consumes around 1% of the world's total energy production leading to about 1.4 % of the world's total energy emissions (Capdevila-Cortada, 2019). That is why it is of importance to design a process which is more sustainable than the processes that currently exist, with a large reduction in  $CO_2$  emissions. This report focuses on comparing different cases and new methods with conventional Haber-Bosch methods in order to find the most sustainable route to produce ammonia.

## List of Abbreviations

SMR	Steam Methane Reforming
LCA	Life Cycle Assessment
LHV	Lower Heating Value
HHV	Higher Heating Value
TRL	Technology Readiness Level
PEM	Proton-Exchange Membrane
ASU	Air Separation Unit
PSA	Pressure Swing Adsorption
HBP	Haber-Bosch Process
HB	Haber-Bosch
NPV	Net Present Value
LCOA	Levelized Cost of Ammonia
Capex	Capital Expenditures
Opex	Operational Expenditures
CEPCI	Chemical Engineering Plant Cost Index
$CO_2$ eq	$CO_2$ equivalent



# 1

## LITERATURE SUMMARY

### 1.1. GREEN ELECTRONS PROCESS

One option is to look at a completely different process to produce ammonia. Recently there has been some progress in electrochemical nitrogen reduction using green electrons according to the following reaction:  $N_2 + 6H^+ + 6e^- \rightarrow 2NH_3$ . This reaction can take place at ambient conditions and could greatly reduce the CO<sub>2</sub> footprint. According to the literature, lithium-metal based methods show one of the highest Faraday Efficiencies (Lazouski *et al.*, 2019) and could potentially lead to methods with higher efficiencies. But overall, there seems to be a large room for improvement, the scales of the reactions are modest and are still in the early stages of development (Martín *et al.*, 2019).

### 1.2. SMR BASED HYDROGEN PRODUCTION

The other option is to look at the way the reactants are provided for the Haber-Bosch process, most importantly at the way hydrogen is produced. Currently steam methane reforming is the most widely used method of hydrogen production and produces about 80-85% of global hydrogen (Simpson and Lutz, 2007), the remaining hydrogen is primarily derived from coal gasification and electrolysis. This process however brings a high carbon footprint due to the formation of carbon monoxide which is converted to carbon dioxide through the water-gas shift reaction. Exergoenvironmental analysis and LCA (Boyano *et al.*, 2011) have concluded that SMR has an environmental impact of 950.7 mPt/kg H<sub>2</sub>, in this scale the eco-indicator (1 Pt) is equal to the yearly environmental impact of an average European citizen.

### 1.3. NUCLEAR BASED HYDROGEN PRODUCTION

As an attempt to lower the environmental impact of ammonia production, other renewable methods of hydrogen production need to be considered. In fig. 1.2, an overview of

selected hydrogen production methods that were analyzed is provided (Acar and Dincer, 2014). Thermochemical water splitting from nuclear energy using Cu-Cl or S-I cycles have shown to be a promising technology in the future. This method uses the heat released from nuclear reactors to drive a series of chemical reactions to realize water decomposition (Xu *et al.*, 2017). The typical flow diagram of the SI cycle is illustrated in fig. 1.1. Cu-Cl cycles have been estimated to reach 40% efficiency while S-I may reach up to 60% efficiency, albeit requiring higher temperatures to operate. When compared to traditional hydrogen producing methods, nuclear cycles perform better on greenhouse warming potential, acidification potential while having a similar production cost. Thermochemical cycles are very promising but still in the research/testing phase, therefore they have a technological readiness level of 3-4. Additionally, the implementation of nuclear energy may be inhibited due to political resistance, particularly in the Netherlands.

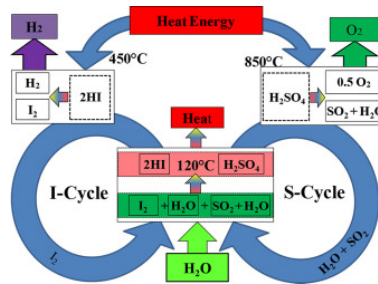


Figure 1.1: Typical flow diagram of an S-I cycle (Xu *et al.*, 2017)

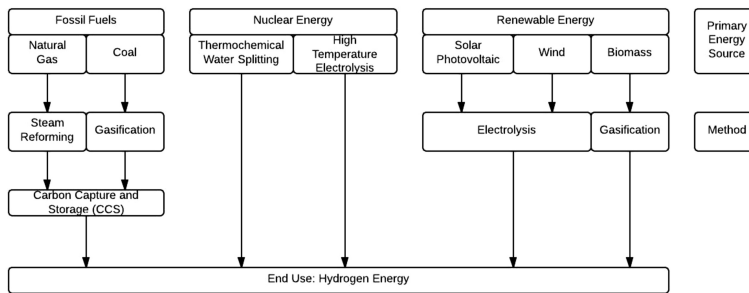


Figure 1.2: Overview of selected hydrogen production methods from different energy sources (Acar and Dincer, 2014)

## 1.4. BIOMASS BASED HYDROGEN PRODUCTION

Another way to produce hydrogen without tapping into fossil fuels is through biomass gasification. This process is similar to coal gasification as it uses pyrolysis and gasification to obtain hydrogen gas. The efficiency of a dual fluidized bed using biomass gasification process may reach up to 69% (LHV based) with prices of 2.7 €/kg according to

Binder *et al.*, 2018. Binder also states that governmental support is necessary to support the implementation of biomass-based hydrogen production, especially in the first 15 years. The use of biomass gasification for hydrogen production has been limited, contemporary plants have primarily used biomass gasification to produce syngas, which is then burned for CHP (combined heat and power) (Jafri *et al.*, 2020). Therefore the TRL for hydrogen production using biomass is around 5-6.

## 1.5. ELECTROLYSIS BASED HYDROGEN PRODUCTION

The last method which was researched to produce hydrogen is through electrolysis. In 2010 only 4% of the hydrogen was produced by electrolysis (Huggins, 2010), mainly because of the higher costs of hydrogen produced by electrolysis (Brauns and Turek, 2020). There are three main types of electrolyzers, namely; alkaline, PEM & solid oxide. Both alkaline and PEM electrolyzers are commercially available, while solid oxide electrolyzers are in the demonstration stage and expected to become fully commercial in 2025-2030 (Banares-Alcantara *et al.*, 2021). Banares also gives a table with different values, like energy consumption and costs, for all three methods. This information is useful when comparing the different methods. The short start-up times of PEM electrolyzers in cold stand-by offers an advantage in the flexible operation, needed in combination with renewable energy sources. However the problem with PEM electrolyzers is the corrosive membrane. These corrosive conditions cause the need for electrodes made of noble metals, which increase the costs of such system (Buttler and Spliethoff, 2018). Buttler also states that Solid oxide electrolyzers are operating at a high temperature, around 700-900 °C. These higher temperatures also increase the efficiency of the system. The drawback is that energy is needed to reach these operating temperatures.

## 1.6. NITROGEN PURIFICATION

Purified Nitrogen is also needed for ammonia production. This can be produced from air by different methods. In the first method, hydrogen is combusted. This method can be used in combination with a solid oxide electrolyzer. The combustion removes oxygen from the air and will generate the heat needed to reach the operating temperature (Banares-Alcantara *et al.*, 2021). Alkaline and PEM electrolyzers will use other technologies, like; an air separation unit (ASU), pressure swing adsorption (PSA) or membrane permeation. Again Banares gives a table, which compares the performance of the three methods. A cryogenic ASU is the most efficient and cost effective technology of producing nitrogen (A. Smith and Klosek, 2001). A PSA system operates well when a steady flow is needed. For fluctuating flows the system will operate at partial capacity, leading to low efficiencies and high operating costs (Ivanova and Lewis, 2012). According to Smith, both a PSA and membrane permeation systems will require an extra deoxygenation system, to increase the quality of the nitrogen.

### 1.7. ELECTRIFIED HABER-BOSCH PROCESS

To create a new process which is completely independent of fossil fuels, the whole process needs to be electrified and certain process optimizations need to be made. C. Smith *et al.*, 2020 state that in order to enable a carbon-free ammonia production, the process needs to be decoupled from SMR, electric compressors need to replace condensing steam turbine compressors and alternative ammonia separation techniques need to be adopted to replace condensing steam turbine compressors. The adoption of these changes can lead to energy efficiency improvements and complete elimination of direct CO<sub>2</sub> emissions.

### 1.8. FEASIBILITY

Finally, the feasibility of producing ammonia by using renewable energies was looked at. Currently, SMR and the Haber-Bosch Process are the most cost-efficient at a levelized cost of ammonia of \$798/ton compared to \$917/ton of ammonia by using on-shore wind energy and alkaline electrolysis for example. Considering the reduction in capital costs, followed by a significant increase in carbon tax in the future (more than \$30/ton of CO<sub>2</sub>), green ammonia can be more economically feasible in the future as the cost of SMR-HBP is estimated to be at \$819/ton of ammonia and at 673 \$/ton using wind to power alkaline electrolyzers and an electric Haber-Bosch Process (Noshervani and Neto, 2021).

### 1.9. CONCLUSION

In conclusion, while the methods used today may seem financially more interesting, the main motivation of this project is to find a method which emits less CO<sub>2</sub> and uses renewable energies, mainly wind and solar energy. The focus will be on replacing SMR for the hydrogen production and designing a completely electrified Haber-Bosch process which can properly function in combination with the intermittent nature of renewable energies. Considering that a reduction of the prices of ammonia production are projected in the future and the high TRL's of electrolysis methods, it seems that making the Haber-Bosch process sustainable could be a possibility in the near future.

# 2

## CONCEPTUAL PROCESS DESIGN

In this chapter, the different steps and decisions made in the process are analyzed and reported. First, the process creation shows principal steps like the synthesis steps and basic design operations. Then the process design is reported and includes the decisions made about the different units of operation and a final qualitative flow sheet. The design process is based on the methods used in chapter 3 and 4 of *Plant Design and Economics for Chemical Engineers* (Peters, 2003) and was adapted to the scope of this project. Finally the source of energy is discussed, taking into consideration the climate goals that have been set for 2030 and 2050.

### 2.1. PROCESS CREATION

This part of the process design involves the decision of various configurations of processing operations including the mode of operation, raw materials and products specifications and the process synthesis.

#### 2.1.1. BATCH VS. CONTINUOUS PROCESS

The first decision that needs to be made when designing any process is the mode of operation. In general, continuous processes are preferred when it comes to the production of chemicals like ammonia (Peters, 2003). Furthermore, processes with chains of high pressure compressors, extensive heat integration and sensitive catalysts cannot be operated outside steady state (C. Smith *et al.*, 2020). Semi-continuous and batch operation by their nature are unsteady state operations, meaning that they cannot be used in this process (Felder *et al.*, 2017). The reason this was looked into is because of the interest in producing hydrogen and nitrogen when energy prices are low, due to the mismatch between supply and demand of renewable energies. If this process is to be operated as a steady state continuous process, hydrogen and nitrogen streams need to be continuously provided.

### 2.1.2. RAW MATERIALS AND PRODUCTS SPECIFICATION

In 2020 Yara, the world's leading ammonia producer joined forces with Danish energy company Ørsted to produce renewable ammonia from wind energy. A 100 MW electrolyzer plant is used to produce hydrogen which is used to produce ammonia. The plant aims to produce 75,000 tons of ammonia per year - approximately 10% of the capacity of one of Yara's Sluiskil plants. This would result in a total reduction of CO<sub>2</sub> emissions by 100,000 tons per year. The plant is projected to be operational by 2024/2025.

One can use this basic value of 75,000 tons of ammonia per year as a stepping stone for further analysis. The flow rate of materials can then be determined assuming the plant runs 365 days per year and 24/7. The flow rate of ammonia is 8.56 tons/h. Assuming no losses, the flow rate of nitrogen and hydrogen calculated through molar balances are 7.04 tons/h and 1.52 tons/h respectively.

After the initial flow rates for nitrogen and hydrogen were set. It seemed necessary to add a purge stream in the recycle stream, in order to ensure a high quality of the nitrogen-hydrogen mixture. Therefore the flow rate becomes 8.03 tons/h. Also the plant will run only 350 days per year, because of the need for maintenance (). This results in a production rate of 67,500 tons of ammonia per year.

The Haber-Bosch process converts gaseous Nitrogen and Hydrogen into gaseous Ammonia at a temperature range between 350 and 550 °C and a pressure range between 150 and 300 bar according to the following reaction :  $N_2 + 3 H_2 \rightarrow 2NH_3$

Figure 2.1 below shows the main materials and product specifications needed for the Haber-Bosch process. This is further explained and analysed in the detailed preliminary design.

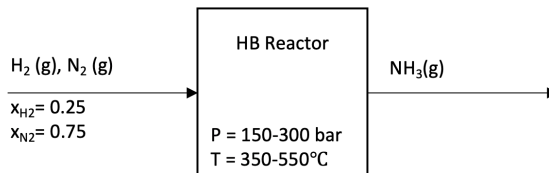


Figure 2.1: Composition of raw materials and product streams, phase, temperature and pressure range of the Haber-Bosch process

### 2.1.3. PROCESS SYNTHESIS

The next step in the process creation is the selection of the basic processing operations to convert the raw materials to the product such as separation of mixture, change in temperature, etc. These steps are summarized in the list below.

1. Demineralisation of water to the right purity for electrolysis: composition change (separation of mixture).
2. Pressurization of water to reach the correct pressure for electrolysis: Pressure difference (change in pressure).

3. Heating of water to reach the correct temperature for electrolysis: Temperature difference (change in temperature).
4. Production of hydrogen from water: Molecular change (chemical reaction).
5. Separation of nitrogen from air: Composition change (separation of mixture).
6. Mixing of hydrogen and nitrogen: Distribution change (mixing of streams).
7. Pressurization of the mixture to the correct pressure for HB: Pressure difference (change in pressure).
8. Heating of the mixture to the correct temperature for HB: Temperature difference (change in temperature).
9. Production of ammonia from nitrogen and hydrogen (Haber-Bosch): Molecular change (chemical reaction).
10. Separation of ammonia from the product stream: Composition change (separation of mixture).
11. Liquefaction of ammonia (liquid ammonia, because that is the desired mode of transportation): Phase difference (phase change).
12. Purge stream to prevent build up of undesired elements in the recycle stream: Composition change (separation of mixture).
13. Mixing the recycle stream with nitrogen and hydrogen (return to step 5): Distribution change (mixing of streams)

## 2.2. PROCESS DESIGN

The process creation serves as a starting point from which the optimal process can be designed. Now that the different synthesis steps have been determined, the function of each unit related to those steps can be determined. From there, the different units of operation can be established to finally be able to set up a quantitative flow sheet with all operations, pressure and temperature as well as work and heat input.

### 2.2.1. FUNCTIONS DIAGRAM

The functions diagram seen in figure 2.2 shows all processes and material flows for each different step. Heat or work flows needed for each step is included as well. Temperature and pressure ranges are also showed for each relevant "box", this is further explained in section 2.2.3 . The red outline in the figure shows the system boundaries for which the material and energy balances will be carried out on in chapter 3.

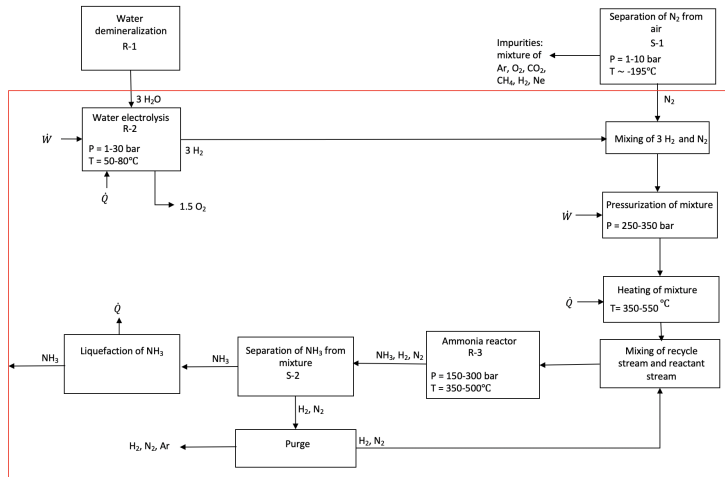


Figure 2.2: Functions diagram of the process including pressure and temperature ranges of different functional units

### 2.2.2. HYDROGEN AND NITROGEN STORAGE FOR STEADY STATE OPERATION

Now that the function diagram has been established, the next step is to decide which different units of operation need to be used for the process. An important aspect of this design is that it needs to function continuously and in a steady state. This can only be done when there is a continuous supply of hydrogen and nitrogen. If the plant is coupled to renewable energy sources like wind energy and solar energy, it will have to be compatible with the intermittent nature of those energy sources.

One option is to look at hydrogen and nitrogen buffers, which means that hydrogen and nitrogen could be produced at times where there is an energy surplus. For wind energy, this means that the storage tanks could be filled at night when there is a mismatch between supply and demand which leads to low energy prices. Which is why the feasibility of storing hydrogen and nitrogen at a large scale was looked into.

Hydrogen storage is very challenging due to its very low density (0.08900 g/L at standard temperature and pressure) (Portarapillo and Benedetto, 2021). According to the calculations in appendix E.4, more than a thousand pressurized tanks or at least 3 massive low pressure storage tanks would be needed to store hydrogen for the plant to operate at this scale. There is also the possibility of storing Hydrogen in salt caverns, but this may lead to purity issues because of the presence of bacteria, which cover 30 percent of the cavern volume and which in the presence of sulfates and carbonates consume hydrogen, producing H<sub>2</sub>S and/ or methane. Salt caverns also pose safety issues in terms of fires, and toxic chemical release and dispersion (Portarapillo and Benedetto, 2021). Furthermore, these salt caverns would also induce a constraint when it comes to plant localization, considering most salt caverns in the Netherlands are situated in Twente (Sodm, 2021).

For Nitrogen, a tank from "Cryolor" made for large industries was taken as a reference for the scale of Nitrogen storage for this process. These models allow a customized storage for liquid Nitrogen with a maximum capacity of 1,000,000 L (Cryolor, 2019).

At a temperature of  $-195\text{ }^{\circ}\text{C}$ , which is the temperature at which Nitrogen leaves the cryogenic distillation unit, liquid Nitrogen has a density of  $760\text{ kg/m}^3$  (EngineeringToolbox, n.d.). For 24 hours of operation, 160,960 kg of Nitrogen needs to be stored, which then corresponds to a storage volume of 222,000 L. This means that it is possible to store Nitrogen and use energy surplus.

So for this process, it was chosen to install nitrogen tanks for storage which can be filled when there is an energy surplus. Producing hydrogen continuously without storage means that it will partly be produced from the energy from the grid, which means that it will have a higher  $\text{CO}_2$  footprint, considering that currently, a large part of this energy comes from fossil fuels. But hydrogen storage at this scale is not possible yet in the near future, so it is a necessary measure for this plant to operate continuously and in steady state.

### 2.2.3. UNITS OF OPERATION AND DETAILED PRELIMINARY DESIGN

The last step in designing the qualitative flowsheet of the process is to define all the units of operation associated to all the boxes in the functions diagram in section 2.2.1, including the particular operating pressure and temperature of each unit.

**Water demineralization** For the water electrolyser, demineralized water is needed to prevent accumulation of minerals in the electrolyser and maintain its proper functioning. Demineralized water is obtained through ion exchange processes to remove almost all ionic mineral contaminants (Marshall, 2018). In a dual bed exchanger, raw water is passed via two polystyrene bead filled (ion exchange resins) beds. The cations get exchanged with hydrogen ions in the first bed and the anions are exchanged with hydroxyl ions in the second one. Mixed-bed exchangers offer a higher water quality compared to dual-bed systems and hold a mixture of different resins housed within a single ion exchange column. But they also require a more involved resin regeneration process, because the resin will become exhausted at an earlier stage and will not be able to facilitate ion exchange reactions (Austrowatertech, n.d.). Considering water quality in alkaline systems is much more tolerant than other water electrolysers like PEM and considering the additional costs associated with frequent resin regeneration, a dual bed exchanger seems to be sufficient for the water quality of this process (Britton, 2018).

**Water Electrolyser** Three different methods of water electrolysis were compared through a multi-criteria analysis; alkaline electrolysis, Proton-exchange membrane and solid-oxide electrolysis, which can be found in appendix A. The MCA shows that alkaline electrolysis is the best option for this project. Alkaline electrolysers can deliver hydrogen at

pressures between 1-30 bar and temperatures around 50-80 °C (Rashid *et al.*, 2015). For the same reason as determined for nitrogen, a pressure of 30 bar is most optimal for this process as this decreases the load on the compressors.

## 2

**Ammonia reactor** Typical operating temperatures for the Haber-Bosch process lie around 350 - 500 °C (Cheema and Krewer, 2018). A low temperature moves the reaction equilibrium to the right, resulting in higher conversion, however the rate of reaction is also low at lower temperatures. A value of 450 °C is chosen for this process; this is low enough such that there is an acceptable yield, and high enough that this reaction takes place at an acceptable rate.

Typical operating pressure for HB is around 150 - 300 bar. The pressure used in plants varies greatly due to differences in design. Changes in number of beds used or in cooling show great changes in steady-state pressure and temperature Khademi and Sabbaghi, 2017. Khadammi and Sabbaghi showed that three bed reactors are most efficient and cost-effective for NH<sub>3</sub> synthesis. The electrified HB-process studied by Cheema and Krewer used a fixed three bed ammonia synthesis reactor with inter-stage cooling, they found a stable operation envelope of 194.32 to 213.91 bar. This operation envelope is due to the temperature range at which the catalyst can operate, higher pressures lead to higher temperatures, with a maximum temperature of 803 K. Therefore the reactor pressure for this design will be 213 bar and a fixed-three bed ammonia reactor will be used.

**Nitrogen Purification** Three different methods of nitrogen purification were compared through a multi-criteria analysis; an air separation unit, pressure-swing adsorption and membrane technology which can be found in appendix A. The MCA shows that an air separation unit, or cryogenic distillation, is the best option for this project, this results in a very pure product of nitrogen. Cryogenic distillation can deliver pressures from 1-10 bar and temperatures around -195 °C (Banares-Alcantara *et al.*, 2021). Higher pressures in the feed stream results in a lower load on the compressor. Therefore a pressure of 10 bar is chosen for nitrogen production. The cryogenic distillation process however is not in the system boundaries. This is due to the complexity of this process which makes modelling a significantly harder challenge. Data from this process step is determined from literature.

**Multi-stage compressor** The mixture of hydrogen and nitrogen has a pressure of 10 bar, which must be pressurised to 213 bar. To accomplish this a multi-stage compressor unit is required. This unit comprises of 4 compressors working at a pressure ratio of 2.148. The multi-stage compressors will have a maximum allowed temperature of 150 °C,

as higher temperatures will result in damaging of the packing. (Palys *et al.*, 2018). Inter-stage cooling of the stream is required to keep the temperatures within an acceptable range. The cooling is provided by water which can be obtained from rivers, dependent on location.

**Heat exchangers** Both heat exchangers in this process (before and after the ammonia reactor) design will be shell-and-tube exchangers which have a relatively simple and economical design as well as high efficiency. An important factor in choosing the heat exchanger type is the pressure. This process runs at 213 bar, so heat exchangers such as double-pipe exchangers and plate exchangers will not suffice at this pressure. A D-type floating head heat exchangers will be most optimal for this use (Brogan, n.d.).

**Refrigeration cycle** A refrigeration cycle is added to facilitate the condensing of ammonia. This is modelled as a vapour-compression refrigeration cycle with isentropic compressors and isobaric heat exchangers. Propylene is used as refrigerant as it shows desirable properties at temperatures at which ammonia condenses (-33°C at 1 atm).

**Purge stream** The purge stream is a portion of the recycle stream that is withdrawn to prevent the buildup of a material that remain in the recycle stream. It is not desirable as it reduces the global conversion of the process, but it is necessary. In this case it is used particularly to prevent buildup of the inert gas Argon from the stream. A purge of 5% is chosen as this showed the best result in ammonia output through iteration.

**Flash separator** The flash separator is to separate the condensed ammonia from the unreacted gaseous hydrogen and nitrogen. The remaining  $N_2$  and  $H_2$  is recycled back to the process. The mixture undergoes a pressure drop of 10 bar in the flash separator, which was determined through an iterative process.

**Recycle compressor** The recycle compressor is to compress the recycled stream recovered from the flash separator back to the desired pressure of 213 bar. This stream is then redirected to the heat exchangers and reactor. The recycle compressor is modeled as an isentropic compressor.

The detailed preliminary design can be seen in figure 2.3 below, which includes all the units of operation.

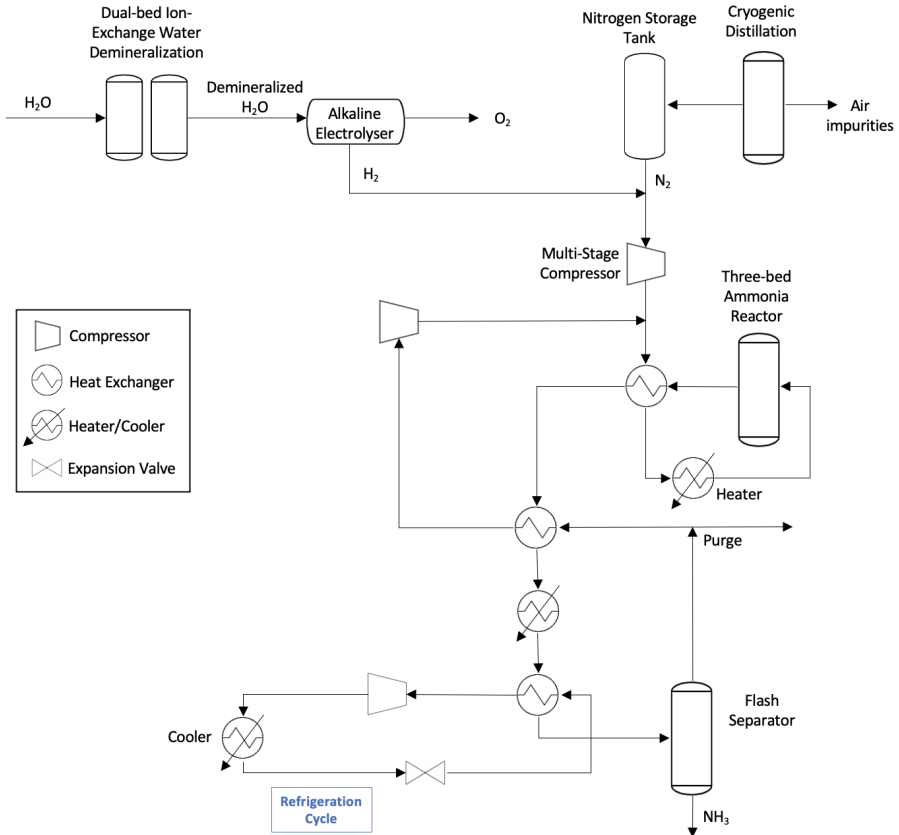


Figure 2.3: Detailed preliminary design including all units of operation of the process

## 2.3. ENERGY SOURCE OF THE PLANT

The ammonia plant needs to continuously function 24/7 and at steady state as stated in section 2.2.2, which means there needs to be a continuous supply of electricity for the plant. This means that the electricity needs to be sourced completely or partly by the national grid in the Netherlands. The consequence is that higher  $CO_2$  emissions are associated to the production of ammonia.

To be able to design the plant with the least amount of  $CO_2$  emissions, two different cases are compared in chapter 5. In the first case, the plant is active in the year 2030 and the energy is sourced completely from the grid. This takes into consideration that 70% of the energy from the grid will come from renewable energy sources in the Netherlands. The second case makes use of a microgrid, meaning the chemical plant will be coupled

to a wind farm and the energy shortages will be complemented by energy from the grid, the grid will be the same as in the first case. The maximum rated power of the wind farm will be equal to the power usage of the renewable process.



# 3

## MASS AND ENERGY BALANCES

In this chapter the mass and energy balances of the process are determined. For the hydrogen electrolysis a Python script is developed, while the ammonia synthesis is modeled using Aspen.

### 3.1. MASS BALANCES

The mass balances for this system are calculated using Aspen Plus. The flowsheet given in figure is modelled in Aspen with an aim to produce 75,000 tonnes of ammonia per year as determined in section 2.1.2.

#### 3.1.1. AMMONIA SYNTHESIS

The Aspen model is based on the flowsheet given in figure B.1. This model however does not contain the water electrolysis due to incompatibility between Aspen's gas processing template and electrolysis. Therefore water electrolysis is calculated separately in section 3.1.2.

The modules contained in the model are: mixers, multi-stage compressors, single compressors, heat exchangers, Gibbs reactors, flash separators, and heaters/coolers. The Peng-Robinson equation of state is used in this model, as this EOS shows more accurate results than the ideal gas law when there is condensation.

#### 3.1.2. HYDROGEN ELECTROLYSIS

The Python script, developed to calculate the mass balance of the hydrogen electrolysis, has the mass flow rate of the produced hydrogen as variable input. When the mass flow rate of hydrogen needed for the ammonia synthesis is known via the Aspen model, the mass flow rate can be converted to a mole flow rate using the mole mass of hydrogen. The mole flow rates of water and oxygen are determined using the stoichiometric values of the electrolysis reaction (3.1).



So for every mole of hydrogen produced; also a halve mole of oxygen is produced and one mole of water is needed. This distribution is also the same for the mole flow rates. These mole flow rates of water and oxygen can be converted back to mass flow rates, again using the mole masses. These mass flow rates have to satisfy the following condition (3.2).

$$\dot{m}_{H_2O} = \dot{m}_{H_2} + \dot{m}_{O_2} \quad (3.2)$$

From the Aspen simulation (app B) is known that the mass flow rate of hydrogen is 1.52 ton/hr. The corresponding results of the Python script and the Python script are included in Appendix C.

3

## 3.2. ENERGY BALANCES

The largest consumers of energy in this process are the electrolyzers, cryogenic distillation, compressors and coolers. The electricity consumed by the electrolyser is discussed in section 3.2.2 and the energy balance for the other components is examined in section 3.2.1.

### 3.2.1. AMMONIA SYNTHESIS

The majority of the energy balances are calculated in Aspen Plus. This includes work required for compressors and heating/cooling necessary for heat exchangers, reactors and separators. The values found in Aspen are validated with formulas from Moran and Shapiro, 2010 and Mills, 2015.

**Compressors** The compressors are modeled as isentropic compressors with an isentropic efficiency of 0.72. This includes the series of multistage compressors used to compress the mixture before entering the heater as well as the recycle compressor. The work required for compression is expressed in equation 3.3 where kinetic and potential energies are neglected.

$$\dot{W} = \dot{m} * (h_{in} - h_{out}) \quad (3.3)$$

**Heat exchangers** The heat exchangers are modeled as isobaric processes and are assumed as producing no work. The first law can then be written as equation 3.4 from Mills, 2015 where kinetic and potential energies are again neglected.

To determine the area required for the heat exchangers, the following equation can be used from Mills (8.18) eq. 3.5. Where  $U$  is the heat transfer coefficient [ $W/m^2K$ ],  $A$  the area of the heat exchanger [ $m^2$ ] and  $\Delta T_{lm}$  the log mean temperature of hot and cold streams eq. 3.6. The subscript '0' is used to denote the temperature of a substream at the start of the heat exchanger and 'L' at the end of the heat exchanger.

$$\dot{Q} = \dot{m}_H * (h_{H,in} - h_{H,out}) = \dot{m}_C * (h_{C,out} - h_{C,in}) \quad (3.4)$$

$$\dot{Q} = U * A * \Delta T_{lm} \quad (3.5)$$

$$\Delta T_{lm} = \frac{(T_H - T_C)_L - (T_H - T_C)_0}{\ln\left[\frac{(T_H - T_C)_L}{(T_H - T_C)_0}\right]} \quad (3.6)$$

The temperatures of the hot and cold streams per heat exchanger are tabulated in table 3.1 with the corresponding heat transfer coefficient, heating/cooling duty and area required. The heat transfer coefficient for gas-to-gas heat transfer ranges between 10-30 W/m<sup>2</sup> K (Mills, 2015) and is assumed to be 30 W/m<sup>2</sup> K for all heat exchangers.

Table 3.1: Substream temperatures, log mean temperatures, heat transfer coefficient, heating duty and required area corresponding with the heat exchangers

	Heat exchanger 1	Heat exchanger 2	Heat exchanger 3
$T_{H0}$ [°C]	450	295.2	20
$T_{HL}$ [°C]	295	186.3	-33
$T_{C0}$ [°C]	140.6	-33	-48.2
$T_{CL}$ [°C]	285	150	-33.4
$\Delta T_{lm}$ [°C]	83.7	133	13.2
$U$ [ $\frac{W}{m^2 K}$ ]	30	30	30
$Q$ [kW]	2646	1850	1513
$A$ [ $m^2$ ]	1053	463	3823

**Reactor** The ammonia synthesis reactor is modeled as an adiabatic and isobaric multi-fixed bed reactor with radial flow. Radial flow reactors allow for small diameter catalyst particles and therefore low pressure drops (Cheema and Krewer, 2018). Heat produced from the exothermic reaction is used to preheat the reactor feed as well as the recycle stream. Normally multi-fixed bed reactors require interstage cooling as large variations in temperature results in faster deactivation catalysts (Sinnott and Towler, 2009). The total cooling duty for the reactor is 7080 kW.

**Additional heating & cooling** Heat from the reactor is used to preheat the reactor feed stream, increasing its temperature to 285 °C. To obtain the necessary temperature of 450 °C an electric impedance heater is used with a heat duty of 3005 kW.

This electrified Haber-Bosch process has four components which require cooling: the multistage compressor, the ammonia synthesis reactor and the ammonia cooling. Cooling for the reactor is achieved through steam generation and is explained in detail in appendix G. Cooling for these processes is done through a cooling tower. The cooling duty for the multistage compressor is: 1609 kW; for the ammonia cooling is: 4660 kW, for the ammonia synthesis reactor is 7008 kW and for the condenser is: 2232 kW. This sums up to a total cooling duty of 15,509 kW.

### 3.2.2. HYDROGEN ELECTROLYSIS

The energy balance of hydrogen electrolysis has also been modeled in python. The minimum energy required for the electrolysis reaction can be found in the following equation 3.7 (Harrison *et al.*, n.d.).



In Alkaline electrolyzers the  $48.6kJ/mol$  of heat is generated by internal resistance, when a current flows through the cell(Harrison *et al.*, n.d.). The reaction could be simplified, so  $285.8kJ/mol$  of electricity is the minimum to make the electrolysis reaction possible. When this number is used in equation 3.8, the cell voltage is equal to  $1.48V$ . This voltage is called the thermo neutral voltage, which is the minimum voltage needed without extra heat being produced. However electrolyzers normally work at voltages between  $1.8 - 2.2V$  (cite).

$$\Delta_r G = 2FE \quad (3.8)$$

When a cell voltage of  $2V$  is taken, the energy used for the electrolysis reaction is equal to  $396kJ/mol$ . When this number is multiplied with the mol flow of water, the power can be determined, in this case  $80MW$ .

$$Q = 2(E_{cell} - E_0)F \quad (3.9)$$

So when the cell voltage is higher than the thermo neutral voltage, extra heat will be produced by the electrolysis cell. This amount of extra heat can be calculated using equation 3.9. The heat production of the electrolysis cell is equal to  $100kJ/mol$ . Which corresponds to  $20MW$ , when multiplied with the mol flow of water.

### 3.3. SIZING AND SCALING

The sizing of key equipment is represented in table 3.2. Certain components such as the reactor, flash separator and nitrogen storage tank required more calculation and are scaled in appendix E.

Table 3.2: Sizing and scaling of key equipment in their relevant units

<b>Equipment</b>	<b>Units for sizing</b>	
Multistage compressor	Power, kW	3176.5
Recycle compressor	Power, kW	84.2
Heat exchanger 1	Area, m <sup>2</sup>	1053
Heat exchanger 2	Area, m <sup>2</sup>	463
Heat exchanger 3	Area, m <sup>2</sup>	3823
Electric impedance heater	Heat duty, kW	3006
Cooling tower	Flow, Litre/s	181
Jacketed reactor agitated	Volume, m <sup>3</sup>	80.2
Flash separator	Mass, kg	41 842
Nitrogen storage tank	Mass, kg	241 865

### 3.4. DETAILED ESTIMATE DESIGN BASED ON MASS AND ENERGY BALANCES

The figures below show the results of the mass and energy balances of the process. Figure 3.1 shows the important molar streams of different flows as well as pressure, temperature and enthalpies. The values have been taken from the model made in Aspen which can be found in Appendix B. Figure 3.2 shows the heat and work inputs needed for the process at different units of operation.

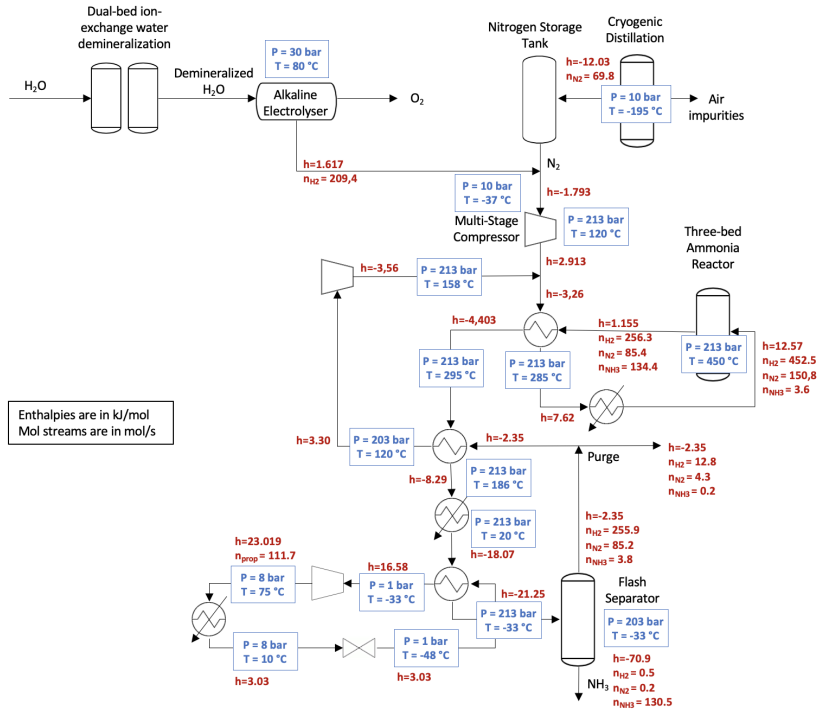


Figure 3.1: Detailed Estimate Design of the process with molar flows, Pressure Temperature and enthalpies of each stream

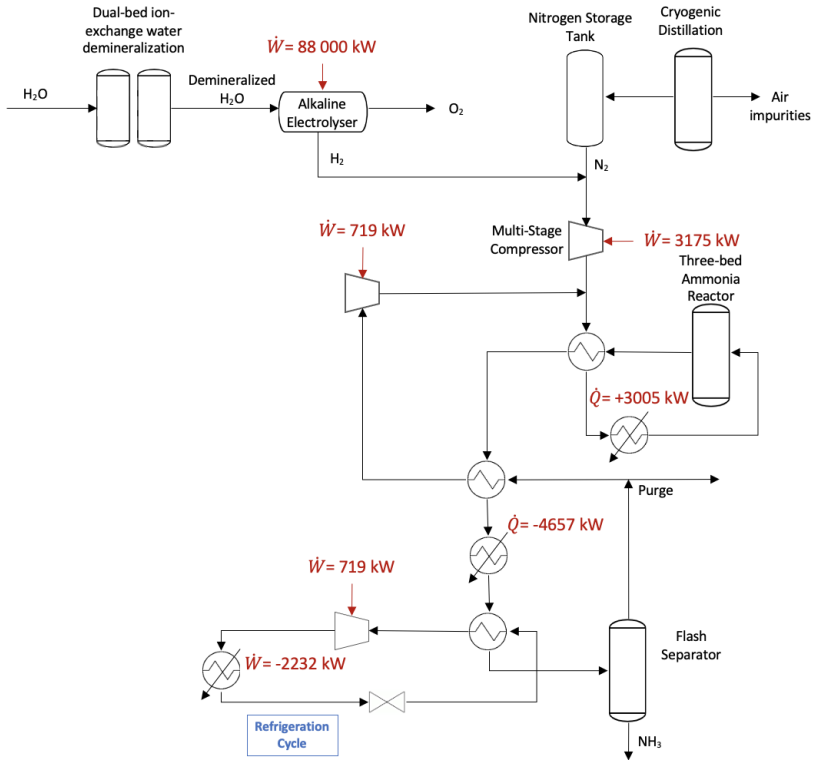


Figure 3.2: Detailed Estimate Design of the process with Heat and work input at different units of operation



# 4

## TECHNO-ECONOMIC ANALYSIS

### 4.1. ELECTRICITY PRICES

The electricity price depends on the different cases. The price of grid electricity is considered first, because it is needed for both cases. According to the CBS the price for electricity in 2019 was 0.072 €/kWh for businesses with a consumption of more than 150,000 MWh per year (CBS, 2021). Because the electricity price is influenced by multiple factors, it is difficult to predict the electricity prices for 2030. However the wholesale electricity price is expected to grow from 0.041 €/kWh in 2019 to 0.051 €/kWh in 2030 (PBL *et al.*, n.d.). When this 25% is also assumed for the retail price, the electricity price will be 0.09 €/kWh in 2030.

For the first case only grid energy is used. From appendix D is known that the total energy consumption is 743.23 GWh per year. This result in a cost of 66.89 million euro.

For the second case also the price of off-shore wind energy is considered. The price for off-shore wind energy consist of multiple factors. The first costs are for the electricity of a wind farm, this is 0.044 €/kWh (NVDE, 2018). On top of that will be 0.015 €/kWh of transmission costs, needed to transport the electricity from off to on-shore (Rekenkamer, 2018). Also 0.00057 €/kWh of energy taxes needs to be added (Belastingdienst, 2021). Resulting in total costs around 0.06 €/kWh.

Considering the second case (Off-shore wind energy + grid) is the most sustainable option and has a lower electricity price, this option is chosen to provide electricity for the process.

From appendix D :

Table 4.1: The different energy sources in case two and the total costs of the energy, data from appendix D

	energy consumption	energy costs
grid	391.23 GWh/y	35.21 million €/y
wind farm	352 GWh/y	21.12 million €/y
total	743.23 GWh/y	56.33 million €/y

## 4.2. CAPITAL COSTS

The capital costs of the ammonia plant constitute of the purchase and installation of the equipment costs. Costing correlations are used to estimate the purchase price of all units of operation. These correlations are obtained from Sinnott and Towler, 2009 which allow for initial cost estimation of various components. These correlations are written in the form of eq. (4.1)

$$C_e = a + b * S^n \quad (4.1)$$

where:

$C_e$  = purchased equipment cost on a U.S. Gulf Coast basis (USGC), Jan 2007. (CEPCI = 509.7)

a, b = cost constants depending on equipment

S = size parameter

n = cost exponent depending on equipment

The purchased equipment cost ( $C_e$ ) in eq. (4.1) is given in \$ in 2007. This cost can be translated to 2020 euros by scaling with the Chemical Engineering Plant Cost Index (CEPCI) from 2020 ( $CEPCI_{2020} = 569.2$ ) and the dollar-euro exchange rate (0.887 as of November 2021) as described in eq. (4.2).

$$C_{e,2020}(\text{€}) = C_{e,2007} * \frac{CEPCI_{2020}}{CEPCI_{2007}} * 0.887 \quad (4.2)$$

### 4.2.1. ELECTROLYSER COSTING

The alkaline electrolyser, used to produce the hydrogen needed for the ammonia production, will have a total power of 88 MW (appendix C). When capital costs of 400 \$/kW are expected in 2030 (in 2020 \$, Christensen, 2020), The capital costs for the electrolyser will be:

$$C_{electrolyser,2020} = 400\$/kW * 88,000kW * 0.887 = \text{€}31,222,400$$

### 4.2.2. COMPRESSOR COSTING

For increasing the pressure of gas streams, reciprocating compressors are used due to their high adiabatic efficiency (Dey, 2021), high maximum discharge pressure and lower cost compared to centrifugal compressors.

The cost parameters for reciprocating compressors are:  $a = 220,000$ ;  $b = 2300$ ;  $n = 0.75$ . This correlation can be used for compressors operating within the range of 93 - 16800 kW of power. The cost estimation for all compressors in the system is given in table 4.2.

Table 4.2: Costs of compressors estimated in 2007 and 2020

Compressor	Power (kW)	Cost, 2007 (€)	Cost, 2020 (€)
1 (multistage)	656	484 505.7261	541 064.6641
2 (multistage)	820	532,638.1934	594 815.8911
3 (multistage)	834	536 663.0986	599 310.6449
4 (multistage)	866	545 688.397	609 389.5146
5 (recycle)	84	276 721.2451	309 024.3922
6 (refrigeration)	330	378 103.8075	422 241.882
7 (refrigeration)	388	398 456.0159	444 969.9122
<b>Total</b>	<b>3979</b>	<b>3 152 776</b>	<b>3 520 816</b>

### 4.2.3. HEAT EXCHANGER COSTING

The total ammonia synthesis process requires three heat exchangers: two for heat recovery from the reactor and one condenser for the refrigeration cycle. D-type floating head heat exchangers are used for this as they are able to withstand high pressures (>150 bar, Brogan, n.d.).

The cost parameters for the heat exchangers are:  $a = 24000$ ,  $b = 46$ ,  $n = 1.2$ . The cost estimation for the heat exchangers is given in table 4.3.

Table 4.3: Cost of heat exchangers estimated in 2007 and 2020

Heat exchangers	Heat/cooling (kW)	Area (m <sup>2</sup> )	Cost (€) 2007	Cost (€) 2020
Exchanger 1	2646.1	632.3	117 707.9	131 448.6
Exchanger 2	1850.6	277.7	58 906.4	65 782.8
Exchanger 3	1513.0	2294.2	463 977.4	518 140.0
<b>Total</b>	<b>6009.7</b>	<b>3204.1</b>	<b>640 591.7</b>	<b>715 371.4</b>

### 4.2.4. REACTOR COSTING

When determining the cost of a reactor it is difficult to obtain an accurate estimation from literature due to the many factors that must be taken into account such as: reactor type, operating temperature, operating pressure, volume, catalyst, etc. To remain consistent with the previous methodology, the cost estimation will be done with Towler and Sinnott's cost correlations for a jacketed agitated reactor. The cost parameters for this reactor are:  $a = 53000$ ,  $b = 28000$ ,  $n = 0.8$ . This correlation can be used for reactors of a volume between 0.5 and 100 m<sup>3</sup>.

$$C_{reactor,2007} = (53000 + (28000)(80.2m^3)^{0.8})(0.887) = \text{€}875,756.43$$

$$C_{reactor,2020} = \text{€}875,756.43 * \frac{569.2}{509.7} = \text{€}977,988.15$$

#### 4.2.5. COOLING TOWER COSTING

The cooling tower will provide the necessary cooling for all components and has a total flow of 181 L/s (table 3.2). Towler & Sinnott give a first impression on the capital costs cooling towers within a flow range of 100 - 10000 L/s. The costs parameters are: a = 150000, b = 1300, n = 0.9.

$$C_{cooling,2007} = (150000 + (1300)(181 \text{ L/s})^{0.9})(0.887) = \text{€}257,151.69$$

$$C_{cooling,2020} = \text{€}257,151.69.2 * \frac{569.2}{509.7} = \text{€}287.170.38$$

#### 4.2.6. ELECTRIC FURNACE COSTING

The ammonia synthesis reactor operates at 450 °C, which is partly achieved through an electric impedance heater with a heating duty of 3 MW. These heaters are commonly used to heat gases, however due to lack of data it is difficult to obtain an accurate evaluation of the cost of such heaters without directly contacting manufacturers. Therefore the T&S cost correlation of a cylindrical furnace is used to estimate the costs. The parameters for this component are: a = 68500, b = 93000, n = 0.8.

$$C_{heater,2007} = (68500 + (93000)(3 \text{ MW})^{0.8})(0.887) = \text{€}259,416.36$$

$$C_{heater,2020} = \text{€}259,416.36 * \frac{569.2}{509.7} = \text{€}289,699.42$$

#### 4.2.7. FLASH SEPARATOR COSTING

The sizing of the flash separator has been thoroughly explained in appendix E.2. The flash drum was modeled as a thin-walled vertical pressure vessel of cylindrical shape with hemispherical caps at both ends made of 304 stainless steel. The shell mass of the pressure vessel is 41,842 kg as given in table 3.2. This allows for the T&S cost correlation for vertical pressure vessels of 304 stainless steel to be used, with cost parameters: a = 15000, b = 68, n = 0.85.

$$C_{flash,2007} = (15000 + (68)(41842 \text{ kg})^{0.85})(0.887) = \text{€}524,754.91$$

$$C_{flash,2020} = \text{€}524,754.91 * \frac{569.2}{509.7} = \text{€}586,012.34$$

#### 4.2.8. NITROGEN STORAGE COSTING

Pressure vessels will be used for nitrogen storage, therefore the same cost correlation can be used as that for the flash separator. The total mass of the shell was calculated in appendix E.3 with data from Cryolor, 2019 and equals 241,865 kg. The cost parameters for vertical pressure vessels of 304 stainless steel are: a = 15000, b = 68, n = 0.85.

$$C_{N_2,2007} = 15000 + (68)(241865 \text{ kg})^{0.85} = \text{€}2,285,625.60$$

$$C_{N_2,2020} = \text{€}2,285,625.60 * \frac{569.2}{509.7} = \text{€}2,552,438.87$$

For other minor equipment and extraneous costs, an additional 10 % of all other equipment costs was added (AIChE, 2019). This represents additional costs of €4,015,189.66

Now that all the purchasing costs of all the units of operation are determined, there are also costs associated with making the equipment fully operational. For this the Lang Factor can be used, which is an estimated ratio of the total installed cost of a process. The Lang factor includes material and labor costs for steel, building, piping, electrical, controls, design and construction costs, etc. These costs however do not include operating costs and the cost of land. The total installed cost (TOT) is obtained by multiplying the appropriate factor  $f$  by the equipment costs:

$$TOT = Equip * f \quad (4.3)$$

For fluid process plants, The Lang factor is  $f= 4.74$ , which means that the total installed costs of this plant in 2020 are €212,309,696.10 (Wolf, 2013).

#### 4.2.9. TOTAL CAPEX

The plant will start construction in 2027 and be operational by 2030. Therefore the costs of 2020 need to be adjusted for inflation in 2027. The inflation from the European Union's monetary policy tends to fluctuate between 1.7% and 2%, an average of 1.85% is used to calculate the costs in 2030 (ECB, 2022) which are tabulated in table 4.4.

Table 4.4: Total capital expenses of all major components, adjusted for inflation to 2027 and taking into account a Lang factor of 4.47

<b>Component(s)</b>	<b>Cost, 2027 Lang factor (€)</b>
Compressors	18 973 568
Heat exchangers	3 855 114
Impedance furnace	1 762 225
Cooling tower	1 649 558
Jacketed agitated reactor	5 306 389
Flash separator	3 168 202
Nitrogen storage	13 765 211
Alkaline electrolyzer	168 256 503
Minor equipment	24 641 085
<b>Total</b>	<b>241 377 654</b>

### 4.3. OPERATIONAL COSTS

Now that the capital costs have been estimated, corresponding to the initial investment of the project, the annual operational costs can now be determined. To determine those costs, the price of utilities, direct production costs, and sales expenses need to be determined (Saeed, 2014).

The price of utilities includes the price of industry water and electricity. Industry water is estimated to cost 0.457 €/m<sup>3</sup> (Zeijden, n.d.) in 2030 considering an annual inflation rate of 1,85 % (O'Neill, 2021). The price of electricity is estimated to cost 0,09 €/ KWh for case 1 (grid energy) and 0,0758 €/ KWh for case 2 as is stated in section 4.1. The following operational costs will be calculated with case 2.

4

#### 4.3.1. OPERATING LABOUR

To estimate the direct production costs, the cost of operating labour is determined first (Jverrett *et al.*, 2020).

$N_{OL}$  = Number of operators per shift

$$N_{OL} = [6.29 + 31.7P^2 + 0.23N_{np}]^{0.5} \quad (4.4)$$

With  $P=0$  (Process steps involving solids)

$N_{np} = 16$  (Other process steps; compression, heating, etc.)

According to the equations above, 4 operators are needed per shift.

$$\# \text{ of operators} = N_{OL} * \frac{\# \text{ Total shifts}}{\# \text{ of shifts per operator}} \quad (4.5)$$

# Shifts per operator = 5 shifts/week \* 49 weeks/year = 245

# Total shifts = 365 days \* 3 shifts/day = 1095

So the total number of operators needed in a year is 18.

For the average salary of a chemical operator in the Netherlands, a salary of 30 6000 €/ year was chosen (Werkenindecemie, 2017), according to salaries in 2021. Which means that the total cost of operating labour is estimated to be 5 508 000 € in a year. With the annual inflation rate of 1,85 %, this corresponds to 6 495 958 € in a year in 2030.

#### 4.3.2. SUMMARY OF OPERATIONAL COSTS

All operational costs summarized below are percentages of either the capital costs, utilities or operating labour (Saeed, 2014). These costs are estimated for the year 2030, these will increase each year with inflation.

Costs aspect	Cost (in €)
Fixed Capital (FC)	241 377 654
Total cost of utilities	57 259 906
Operating Labour (OL)	6 495 958
Maintenance (7.5% of FC)	18 103 339
Miscellaneous materials (10% of Maintenance)	1 810 334
Laboratory costs (21.5% of OL)	1 396 631
Supervision (20% of OL)	1 299 192
Plant overheads (50% of OL)	3 247 979
Capital charges (10% of FC)	24 137 785
Insurance (10% of FC)	24 137 785
Royalties (10% of FC)	24 137 785
Direct production costs (Sum of all costs above, excl. FC)	162 026 695
Sales expenses (SE, 25% of direct production costs)	40 506 674
<b>Total production costs (Production costs + SE)</b>	<b>202 533 369</b>

#### 4.4. NPV CALCULATION

The net present value of the plant was determined over a 25-year lifetime, which is the minimum lifetime of a chemical plant (W. David Smith, 1999). It was assumed that the plant would be fully operational after 3 years of construction and that sales do not begin before it is fully assembled. In the NPV analysis, the capital expenditures are spread over the first three years. The formula for the NPV can be seen below (Khan and Jain, 2000).

$$NPV = \sum_n \frac{CF_n}{(1+i)^n} \quad (4.6)$$

With  $i$  = acceptable rate of return, taken here to be 8% (AIChE, 2019).  $n$  = years, and  $CF_n$  = Cash Flow.

$$CF_n = \frac{P_n}{(1-t_n)} + D_n \quad (4.7)$$

With  $D = I_0 - I_d$  = total depreciation,  $I_0$  = Investment in production facility and support infrastructure (Capital costs). The demolition value  $I_d$  is often neglected, so  $D = I_0$  (Jong, 2021). In this analysis it is taken as a negative value spread over the first three years.

$P_n$  is the annual profit of the plant,

$$P_n = \frac{S_n - C_n}{1-t_n} \quad (4.8)$$

The annual sales  $S_n$  are first estimated by looking at the current price of ammonia in

Europe, which is 1,12 \$/kg NH<sub>3</sub> (0,98 €/kg NH<sub>3</sub>) (Garg, 2021). With the inflation rate in 2030, this price corresponds to 1,16 €/kg NH<sub>3</sub>, so  $S_n = 77\,952\,000$ .  $C_n$  are the total production costs as calculated in section 4.3.2.

The relative tax on profit levels is 25 % in the Netherlands, so  $t_n = 0,25$ . (AZ, 2021).

The NPV was calculated for each year, for a lifetime of 25 years. With a sales price of 1,16 €/kg NH<sub>3</sub> and an electricity price of 0,0758 €/kWh, the NPV is never positive, which means the plant is not able to make a profit with these prices. The results of the NPV calculation can be found in Appendix F.

By trial and error, it seems that to be able to be profitable with the same electricity price, a sales price of 3,15 €/kg NH<sub>3</sub> is needed, which is almost 3x times the estimated price of NH<sub>3</sub>. In this case, the NPV is positive in 2053 and has a value of 5 782 373 €.

Again, by trial and error, with a more acceptable sales price of 2,5 €/kg NH<sub>3</sub>, the electricity price would need to be 0,025 €/kWh. In this case the NPV is positive in 2048 and has a value of 9 872 396 €.

There seems to be no electricity price for which the sales price of 1,16 €/kg NH<sub>3</sub> can be maintained, which means the chemical plant would not be able to be profitable without subsidies on the electricity price. The results of the NPV calculations above can be found in Appendix F.

#### 4.5. LEVELIZED COST OF AMMONIA

The levelized cost of Ammonia is the cost of producing ammonia per kg of product. It is calculated with the formula below for the year 2030. The formula is based on the LCOE (Levelized Cost of Electricity).

$$LCOA = \frac{\sum_n \frac{Opex+Capex}{(1+r)^n}}{\sum_n \frac{Prod}{(1+r)^n}} \quad (4.9)$$

$r$ = discount rate= 10,5 % (Average value) (Grana, 2021),  $Prod$ = production in year  $n$ ,  $n$ = lifetime of the plant= 1 (2030 is the first year that operation begins).

The LCOA in 2030 is 6,52 €/ kg NH<sub>3</sub> with an electricity price of 0,025 €/kWh. The current LCOA in 2021 of NH<sub>3</sub> using current Haber-Bosch methods is 0,798 \$/ kg NH<sub>3</sub> with inflation (Noshervani and Neto, 2021). This corresponds to an LCOA of 0,83 €/ kg NH<sub>3</sub> with inflation in 2030. Which means that this process costs at least 7 times as much as current methods used for ammonia production.

# 5

## COMPARISON OF CO<sub>2</sub> EMISSIONS

### 5.1. CO<sub>2</sub> INTENSITY

In order to determine the CO<sub>2</sub> emissions of the electricity used in the process, the CO<sub>2</sub> intensity of the electricity needs to be known. For both cases the CO<sub>2</sub> intensity of the grid is necessary. In 2030 the dutch government has planned to have 70% of all electricity from renewable sources (EZK, 2021). This will result in a CO<sub>2</sub> intensity of 0.13 kg CO<sub>2</sub> eq/kWh for grid energy in 2030.

The LCA of a German wind farm, comparable in size to the planned 88 MW wind farm and on the north sea, will have a CO<sub>2</sub> intensity of 0.032 kg CO<sub>2</sub> eq/kWh (Wagner *et al.*, 2011). The total CO<sub>2</sub> emissions per kg H<sub>2</sub>, with a ammonia production rate of 67,500 ton per year, are in table 5.1.

Table 5.1: CO<sub>2</sub> emissions of the two cases.

case	source	energy consumption	CO <sub>2</sub> emissions	CO <sub>2</sub> emissions
1	grid	743.23 GWh/y	96,620 ton CO <sub>2</sub> eq/y	1.43 ton CO <sub>2</sub> eq/ ton NH <sub>3</sub>
2	grid	391.23 GWh/y	50,860 ton CO <sub>2</sub> eq/y	0.75 ton CO <sub>2</sub> eq/ ton NH <sub>3</sub>
	wind farm	352 GWh/y	11,264 ton CO <sub>2</sub> eq/y	0.17 ton CO <sub>2</sub> eq/ ton NH <sub>3</sub>
	total	743.23 GWh/y	62,124 ton CO <sub>2</sub> eq/y	0.92 ton CO <sub>2</sub> eq/ ton NH <sub>3</sub>

### 5.2. COMPARISON CONVENTIONAL HABER-BOSCH PROCESS

Now the two cases for a renewable process will be compared to the conventional Haber-Bosch process with SMR.

#### 5.2.1. HYDROGEN PRODUCTION

The main difference between the renewable process en conventional process is the hydrogen production. The emissions per ton produced hydrogen and the emissions per

year, if 12,768 ton hydrogen is required per year, can be found in table 5.2.

Table 5.2: CO<sub>2</sub> emissions per ton H<sub>2</sub> production and total emissions with 12,768 ton H<sub>2</sub> production per year.

	emissions per ton H <sub>2</sub> produced	emissions per year
conventional	10.1 ton CO <sub>2</sub> eq/ton H <sub>2</sub>	128,957 ton CO <sub>2</sub> eq
case 1	6.9 ton CO <sub>2</sub> eq/ton H <sub>2</sub>	88,225 ton CO <sub>2</sub> eq
case 2	4.4 ton CO <sub>2</sub> eq/ton H <sub>2</sub>	56,726 ton CO <sub>2</sub> eq

The emissions of the SMR process are more than to 10 ton CO<sub>2</sub> eq/ton H<sub>2</sub> (Tenhumberg and Bükler, 2020). While the renewable process potentially has less than halve of that.

### 5.2.2. REGENERATION

The heat, produced by the reactor, could be used to power a turbine, so energy could be recovered from the process. Calculations on this turbine can be found in appendix G. From these calculations is known that the electrical power produced by the turbine is equal to 542 kW. The electricity produced can be used in the process and thus lower the energy consumption

A power output of 542 kW, will result in 4,55 GWh per year. In both cases the use of grid energy will be lowered. This means that the emissions will lower with 592 ton CO<sub>2</sub> eq per year. This means that the emissions per ton NH<sub>3</sub> will be reduced to 1.42 ton CO<sub>2</sub> eq/ton NH<sub>3</sub> for case 1 and 0.91 ton CO<sub>2</sub> eq/ton NH<sub>3</sub> for case 2.

### 5.2.3. AMMONIA PRODUCTION

The conventional Haber-Bosch process produces about 2.0 ton CO<sub>2</sub> eq/ton NH<sub>3</sub> (Rouwenhorst *et al.*, 2021). This means that case 1 will reduce the CO<sub>2</sub> emissions by 29%. While case 2 is even able to reduce the CO<sub>2</sub> by 55%.

# 6

## DISCUSSION

This section will discuss the assumptions that have been made regarding the design of the plant and improvements that can be applied to the process.

The techno-economic analysis concluded that the production of ammonia through electrolysis is not profitable given current ammonia and electricity prices. This is mainly due to the high electricity demand of electrolysis coupled with soaring electricity prices in the Netherlands as well as the high capital costs associated with electrolyzers. One may consider the costs of electrolyzers to lower in the future due to increasing innovation in the industry on the basis of learning curves. Another way to lower costs is to situate the plant in a different country with lower (renewable) electricity prices. This may significantly reduce operational expenses while having little influence on CAPEX. Nonetheless further feasibility study needs to be done to accurately determine this.

The variables for the financial model in the techno-economic analysis were obtained from literature and adjusted for inflation in 2030. To accurately determine variables such as electricity prices, ammonia prices, labour costs etc. in the future shows great difficulty and therefore there is a large error margin in these variables. To improve the validity of this model a detailed sensitivity analysis should be made in which changes of variables such as electricity and ammonia prices are taken into account.

These variables are also heavily influenced by change in the political landscape. Policies such as a carbon tax would make ammonia synthesis from electrolysis significantly more cost-effective (Noshervani and Neto, 2021).

The CO<sub>2</sub> intensity calculated for case 1 was done considering the energy-related target goals for 2030 (70% renewable energy). If these goals are not met, the CO<sub>2</sub> intensity should change. Additionally improvements in the grid beyond 2030 will also lower CO<sub>2</sub> emissions. If this plant was to be located somewhere else these emissions should also change.

Case 2 considers a wind park with a capacity of 88 MW to supply energy for the ammonia synthesis. This was considered under the assumption that new windparks are to be opened (Rijksoverheid, n.d.). However the feasibility regarding location and permits are yet to be studied and is a priority for future assessments.

Other improvements in the process can be made in the heat integration. Currently heat from the reactor is used to preheat different ammonia feed streams. Despite that a more rigorous analysis for heat recovery through pinch analysis should be done to optimise all heating and cooling demand within the process.

The ammonia synthesis reactor is multi fixed bed reactor, however due to lack of literature on the economics of such reactors the cost estimation was done for an agitated jacketed reactor. Therefore the calculated cost may deviate from the real reactor. This is likewise the case with the heater component, as the heater is designed as an electric impedance heater but due to lack of data the cost correlation of a cylindrical furnace was used.

The inclusion of a purge is present to remove any buildup of inert gases in the process, mainly Argon. However to add Argon in the Aspen model lead to many convergence errors and therefore had to be omitted in the model. Given more time and experience in Aspen this error should be corrected.

When comparing energy consumption of this process with Haber Bosch processes, this process requires 50% more energy. The current energy consumption of a Haber-Bosch process is 26 GJ/ton  $\text{NH}_3$  (Rouwenhorst *et al.*, 2021) and this process including electrolysis consumes around 39.6 GJ/ton  $\text{NH}_3$ . This increase in energy however does not have a large impact on global warming potential considering it is primarily renewable energy.

# 7

## CONCLUSION

The goal of this report is to design an ammonia synthesis process which is more sustainable than current Haber-Bosch processes. This was done by electrifying the process in which the hydrogen production method was changed from steam methane reforming to water electrolysis. Additionally the generation of nitrogen is done through cryogenic distillation. This results in significant reductions in carbon emissions due to the removal of dependence on natural gas and coals. This new process will reduce total CO<sub>2</sub> emissions by 55%, from 2.0 ton CO<sub>2</sub> eq/ton NH<sub>3</sub> to 0.92 ton CO<sub>2</sub> eq/ton NH<sub>3</sub>. However this electrified process also presents substantially higher costs. This is mainly due to the high capital costs associated with an alkaline electrolyzer and the soaring electricity prices in the Netherlands. The plant is assumed to be operational by 2030 and for it to be profitable it would have to sell ammonia at a price of 3,15 €/kg NH<sub>3</sub>, which is almost triple the current market price if it were to be adjusted for inflation (1,16 €/kg NH<sub>3</sub>). If an electricity price of €0,025/kWh is chosen with an ammonia price of 2,50 €/kg NH<sub>3</sub>, the project will be profitable after 18 years of operation. There is no electricity price at which this process is profitable with current electricity prices.

From an environmental standpoint this new process has great benefits, however in its current state it is simply not economically viable. It must be noted that these costs may be reduced in the future due to increasing innovation in the electrolyzer industry through learning curves which would result in lower costs. Additionally the Haber-Bosch process has seen optimization since the first decade of the 20th century, ammonia synthesis with electrolysis has yet to see commercialization. Therefore there is notable room for process improvement.

Possible options to lower costs are: More extensive heat integration; changing location to a country with lower (renewable) electricity prices; changes in climate policy through subsidies and carbon tax, which would allow the renewable process to be competitive with mainstream ammonia plants.



# 8

## BIBLIOGRAPHY

- Acar, C. and Dincer, I. (2014). "Comparative assessment of hydrogen production methods from renewable and non-renewable sources". In: *International Journal of Hydrogen Energy* 39.1, pp. 1–12. DOI: [10.1016/j.ijhydene.2013.10.060](https://doi.org/10.1016/j.ijhydene.2013.10.060).
- AIChE (2019).
- Austrowatertech, a. (n.d.). *Demineralization Plant*. URL: <https://austrowatertech.com/services/demineralization-plant/>.
- AZ (Aug. 2021). *Corporate income tax*. URL: <https://www.government.nl/topics/taxation-and-businesses/corporation-tax#:~:text=Corporate%20income%20tax%20rates%20in%202021&text=If%20the%20taxable%20amount%20is,taxable%20amount%20exceeding%20%E2%82%AC%20245,000..>
- Banares-Alcantara, R., Valera-Medina, A., Rouwenhorst, K. H. R., Krzywda, P. M., and Leferts, L. (2021). "Chapter 4 - Ammonia Production Technologies". In: *Techno-economic challenges of green ammonia as an energy vector*. Academic Press, pp. 41–83.
- Belastingdienst (Dec. 2021). *Tabellen Tarieven Milieubelastingen*. URL: [https://www.belastingdienst.nl/wps/wcm/connect/bldcontentnl/belastingdienst/zakelijk/overige\\_belastingen/belastingen\\_op\\_milieugrondslag/tarieven\\_milieubelastingen/tabellen\\_tarieven\\_milieubelastingen](https://www.belastingdienst.nl/wps/wcm/connect/bldcontentnl/belastingdienst/zakelijk/overige_belastingen/belastingen_op_milieugrondslag/tarieven_milieubelastingen/tabellen_tarieven_milieubelastingen).
- Binder, M., Kraussler, M., Kuba, M., and Luisser, M. (Dec. 2018). *Hydrogen from biomass gasification*. URL: <https://www.ieabioenergy.com/blog/publications/hydrogen-from-biomass-gasification/>.
- Boiler and condenser pressures - rankine cycle* (Nov. 2021). URL: <https://www.nuclear-power.com/nuclear-engineering/thermodynamics/thermodynamic-cycles/rankine-cycle-steam-turbine-cycle/boiler-and-condenser-pressures-rankine-cycle/>.
- Boyano, A., Blanco-Marigorta, A., Morosuk, T., and Tsatsaronis, G. (2011). "Exergoenvironmental analysis of a steam methane reforming process for hydrogen production". In: *Energy* 36.4, pp. 2202–2214. DOI: [10.1016/j.energy.2010.05.020](https://doi.org/10.1016/j.energy.2010.05.020).
- Brauns, J. and Turek, T. (Feb. 2020). *Alkaline water Electrolysis powered by renewable Energy: A review*. URL: <https://doi.org/10.3390/pr8020248>.

- Britton, B. (Feb. 2018). *In hydrogen production from water electrolysis, what is the water quality? how to treat tap water to suit the electrolyzer?*
- Brogan, R. (n.d.). *Shell and tube heat exchangers*. URL: <https://thermopedia.com/content/1121/>.
- Burhan Kabir Suhan, M., Naimur Rahman Hemal, M., Shoukat Choudhury, M., and Ali Akkas Mazumder, M. (2022). “Optimal design of ammonia synthesis reactor for a process industry”. In: *Journal of King Saud University - Engineering Sciences* 34.1, pp. 23–30. DOI: [10.1016/j.jksues.2020.08.004](https://doi.org/10.1016/j.jksues.2020.08.004).
- Buttler, A. and Spliethoff, H. (2018). “Current status of water electrolysis for energy storage, grid balancing and sector coupling via power-to-gas and power-to-liquids: A review”. In: *Renewable and Sustainable Energy Reviews* 82, pp. 2440–2454. DOI: [10.1016/j.rser.2017.09.003](https://doi.org/10.1016/j.rser.2017.09.003).
- Capdevila-Cortada, M. (2019). “Electrifying the Haber–Bosch”. In: *Nature Catalysis* 2.12, pp. 1055–1055. DOI: [10.1038/s41929-019-0414-4](https://doi.org/10.1038/s41929-019-0414-4).
- CBS (Dec. 2021). *Aardgas en elektriciteit, Gemiddelde Prijzen Van Eindverbruikers*. URL: <https://www.cbs.nl/nl-nl/cijfers/detail/81309NED>.
- Cheema, I. I. and Krewer, U. (2018). “Operating envelope of Haber–Bosch process design for power-to-ammonia”. In: *RSC Advances* 8.61, pp. 34926–34936. DOI: [10.1039/c8ra06821f](https://doi.org/10.1039/c8ra06821f).
- Christensen, A. (June 2020). *Assessment of Hydrogen Production Costs from Electrolysis: United States and Europe*. URL: [https://theicct.org/sites/default/files/publications/final\\_icct2020\\_assessment\\_of%20hydrogen\\_production\\_costs%20v2.pdf](https://theicct.org/sites/default/files/publications/final_icct2020_assessment_of%20hydrogen_production_costs%20v2.pdf).
- Cryolor (Sept. 2019). *Air gas cryogenic storage*. URL: <https://www.cryolor.com/air-gas-cryogenic-storage>.
- Dey, A. K. (Dec. 2021). *Difference between centrifugal and reciprocating compressor (pdf)*. URL: <https://whatispiping.com/centrifugal-vs-reciprocating-compressor/>.
- DoE (July 2016). *Steam Turbine - Department of Energy*. URL: <https://www.energy.gov/sites/prod/files/2016/09/f33/CHP-Steam%5C%20Turbine.pdf>.
- ECB (2022). *Inflation in the Euro Area*. URL: [https://ec.europa.eu/eurostat/statistics-explained/index.php?title=Inflation\\_in\\_the\\_euro\\_area](https://ec.europa.eu/eurostat/statistics-explained/index.php?title=Inflation_in_the_euro_area).
- Energy.gov (n.d.). *Electric resistance heating*. URL: <https://www.energy.gov/energysaver/electric-resistance-heating>.
- EngineeringToolbox (n.d.). *Nitrogen - Density and Specific Weight vs. Temperature and Pressure*. URL: [https://www.engineeringtoolbox.com/nitrogen-N2-density-specific-weight-temperature-pressure-d\\_2039.html](https://www.engineeringtoolbox.com/nitrogen-N2-density-specific-weight-temperature-pressure-d_2039.html).
- EPA (Mar. 2015). *Catalog of CHP Technologies, section 4. technology ...* URL: [https://www.epa.gov/sites/default/files/2015-07/documents/catalog\\_of\\_chp\\_technologies\\_section\\_4.\\_technology\\_characterization\\_-\\_steam\\_turbines.pdf](https://www.epa.gov/sites/default/files/2015-07/documents/catalog_of_chp_technologies_section_4._technology_characterization_-_steam_turbines.pdf).
- EZK (Mar. 2021). *Klimaataakkoord | Elektriciteit*. URL: <https://www.klimaataakkoord.nl/elektriciteit>.
- Felder, R. M., Rousseau, R. W., and Bullard, L. G. (2017). *Felders elementary principles of chemical processes*. John Wiley a Sons.

- Garg, V. (Dec. 2021). *Global ammonia prices surge on European natural gas cost push*. URL: <https://www.spglobal.com/platts/en/market-insights/latest-news/energy-transition/121621-global-ammonia-prices-surge-on-european-natural-gas-cost-push>.
- Grana, P. (Sept. 2021). *Demystifying LCOE*. URL: <https://www.renewableenergyworld.com/solar/demystifying-lcoe/#gref>.
- Harrison, K. W., Remick, R., Martin, G. D., and Hoskin, A. (n.d.). *Hydrogen production: Fundamentals and case study summaries ...* URL: <http://www.nrel.gov/docs/fy10osti/48269.pdf>.
- Huggins, R. A. (2010). *Energy storage*. Springer.
- Ivanova, S. and Lewis, R. (June 2012). *Reactions and separations producing nitrogen via pressure ...* URL: [http://www.airproducts.co.id/~media/Files/PDF/products/producing-nitrogen-via-psa-CEP-Article\\_20120638.pdf](http://www.airproducts.co.id/~media/Files/PDF/products/producing-nitrogen-via-psa-CEP-Article_20120638.pdf).
- Jafri, Y., Waldheim, L., and Lundgren, J. (Dec. 2020). *Emerging Gasification Technologies for Waste Biomass*. URL: [https://www.ieabioenergy.com/wp-content/uploads/2021/02/Emerging-Gasification-Technologies\\_final.pdf](https://www.ieabioenergy.com/wp-content/uploads/2021/02/Emerging-Gasification-Technologies_final.pdf).
- Jong, W. de (2021). *Lecture notes Energy Storage*.
- Jverrett, Qiao, R., and Barghout, R. A. (Aug. 2020). *Cost of Operating Labour*. URL: <https://pressbooks.bccampus.ca/chbe220/chapter/cost-of-operating-labour/>.
- Khademi, M. H. and Sabbaghi, R. S. (2017). "Comparison between three types of ammonia synthesis reactor configurations in terms of cooling methods". In: *Chemical Engineering Research and Design* 128, pp. 306–317. DOI: [10.1016/j.cherd.2017.10.021](https://doi.org/10.1016/j.cherd.2017.10.021).
- Khan, M. Y. and Jain, P. K. (2000). *Theory and problems in financial management*. Tata McGraw-Hill.
- Lazouski, N., Schiffer, Z. J., Williams, K., and Manthiram, K. (2019). "Understanding Continuous Lithium-Mediated Electrochemical Nitrogen Reduction". In: *Joule* 3.4, pp. 1127–1139. DOI: [10.1016/j.joule.2019.02.003](https://doi.org/10.1016/j.joule.2019.02.003).
- Marshall, K. (Nov. 2018). *What Is Water Demineralization and How Does It Work?* URL: <https://www.samcotech.com/what-is-demineralization-and-how-does-it-work/>.
- Martín, A. J., Shinagawa, T., and Pérez-Ramírez, J. (2019). "Electrocatalytic Reduction of Nitrogen: From Haber-Bosch to Ammonia Artificial Leaf". In: *Chem* 5.2, pp. 263–283. DOI: [10.1016/j.chempr.2018.10.010](https://doi.org/10.1016/j.chempr.2018.10.010).
- Mills, A. F. (2015). *Basic heat and mass transfer*. Prentice Hall.
- Moran, M. J. and Shapiro, H. N. (2010). *Fundamentals of Engineering Thermodynamics: Appendices-tables in SI units and English units*. John Wiley amp; Sons.
- Muller-Steinhagen, H. M. G. (Feb. 2011). *Rankine cycle*. URL: <https://thermopedia.com/content/1072/>.
- Noshierwani, S. A. and Neto, R. C. (2021). "Techno-economic assessment of commercial ammonia synthesis methods in coastal areas of Germany". In: *Journal of Energy Storage* 34, p. 102201. DOI: [10.1016/j.est.2020.102201](https://doi.org/10.1016/j.est.2020.102201).
- NVDE (June 2018). *Kosten van Stroom uit wind en Zon Gaan richting die van kolen en gas*. URL: <https://www.nvde.nl/nvdeblogs/kosten-stroom-wind-en-zon-gaan-richting-kolen-en-gas/>.

- O'Neill, A. (Nov. 2021). *European Union inflation rate*. URL: <https://www.statista.com/statistics/267908/inflation-rate-in-eu-and-euro-area/>.
- Palys, M., McCormick, A., Cussler, E., and Daoutidis, P. (2018). "Modeling and optimal design of absorbent enhanced ammonia synthesis". In: *Processes* 6.7, p. 91. DOI: [10.3390/pr6070091](https://doi.org/10.3390/pr6070091).
- PBL, RIVM, CBS, RVO, and TNO (n.d.). *Netherlands climate and Energy Outlook 2020 - summary*. URL: <https://www.pbl.nl/sites/default/files/downloads/pbl-2020-netherlands-climate-and-energy-outlook-2020-summary-4299.pdf>.
- Peters, M. S. (2003). *Plant design and economics for chemical engineers*. McGraw-Hill.
- Portarapillo, M. and Benedetto, A. D. (2021). "Risk Assessment of the Large-Scale Hydrogen Storage in Salt Caverns". In: *Energies* 14.10, p. 2856. DOI: [10.3390/en14102856](https://doi.org/10.3390/en14102856).
- Rankine cycle - steam turbine cycle: Characteristics* (Nov. 2021). URL: <https://www.nuclear-power.com/nuclear-engineering/thermodynamics/thermodynamic-cycles/rankine-cycle-steam-turbine-cycle/>.
- Rashid, M. M., Al Mesfer, M. K., Naseem, H., and Danish, M. (2015). "Hydrogen production by water electrolysis: A review of alkaline water electrolysis, PEM water electrolysis and high temperature water electrolysis". In: *Int J Eng Adv Technol* 4.3. Cited By :150, pp. 80–93. URL: [www.scopus.com](http://www.scopus.com).
- Rekenkamer, A. (Sept. 2018). *Focus op Kosten Windenergie op zee*. URL: <https://www.rekenkamer.nl/publicaties/rapporten/2018/09/27/focusonderzoek-kosten-van-windparken-op-zee>.
- Rijksoverheid (n.d.). *Waar Staan en Komen de Windparken op zee?* URL: <https://windopzee.nl/onderwerpen/wind-zee/waar/>.
- RoadstoHy2 (Apr. 2013). *Large Hydrogen Underground Storage*.
- Rouwenhorst, K., Krzywda, P., Benes, N., Mul, G., and Lefferts, L. (2021). "Ammonia Production Technologies". In: *Techno-Economic Challenges of Green Ammonia as an Energy Vector*, pp. 41–83. DOI: [10.1016/b978-0-12-820560-0.00004-7](https://doi.org/10.1016/b978-0-12-820560-0.00004-7).
- RVO (2016). *Windenergie op zee - rvo*. URL: <https://www.rvo.nl>.
- Saeed, W. (May 2014). *ESTIMATION OF OPERATING COSTS*. URL: <https://chemicalprojects.net/2014/05/11/estimation-of-operating-costs/>.
- Simpson, A. and Lutz, A. (2007). "Exergy analysis of hydrogen production via steam methane reforming". In: *International Journal of Hydrogen Energy* 32.18, pp. 4811–4820. DOI: [10.1016/j.ijhydene.2007.08.025](https://doi.org/10.1016/j.ijhydene.2007.08.025).
- Sinnott, R. and Towler, G. (2009). *Chemical Engineering Design*. Elsevier.
- Smith, A. and Klosek, J. (2001). "A review of air separation technologies and their integration with energy conversion processes". In: *Fuel Processing Technology* 70.2, pp. 115–134. DOI: [10.1016/s0378-3820\(01\)00131-x](https://doi.org/10.1016/s0378-3820(01)00131-x).
- Smith, C., Hill, A. K., and Torrente-Murciano, L. (2020). "Current and future role of Haber–Bosch ammonia in a carbon-free energy landscape". In: *Energy Environmental Science* 13.2, pp. 331–344. DOI: [10.1039/c9ee02873k](https://doi.org/10.1039/c9ee02873k).
- Sodm (May 2021). *Zoutwinning*. URL: <https://www.sodm.nl/sectoren/zoutwinning>.
- Tenhumberg, N. and Büker, K. (2020). "Ecological and economic evaluation of hydrogen production by different water electrolysis technologies". In: *Chemie Ingenieur Technik* 92.10, pp. 1586–1595. DOI: [10.1002/cite.202000090](https://doi.org/10.1002/cite.202000090).

- W. David Smith, J. (1999). *Impact of advances in computing and communications technologies on chemical science and technology report of a workshop*. National Academy Press.
- Wagner, H.-J., Baack, C., Eickelkamp, T., Epe, A., Lohmann, J., and Troy, S. (2011). “Life cycle assessment of the offshore wind farm alpha ventus”. In: *Energy* 36.5, pp. 2459–2464. DOI: [10.1016/j.energy.2011.01.036](https://doi.org/10.1016/j.energy.2011.01.036).
- Werkenindechemie (Nov. 2017). *Werkenindechemie - Salaris van de verschillende functies binnen chemie*. URL: <https://werkenindechemie.nl/salaris-chemie/>.
- Wikipedia (Jan. 2022). URL: <https://en.wikipedia.org/wiki/Iron>.
- Wischnewski, B. (n.d.). URL: [http://www.peacesoftware.de/einigewerte/calc\\_dampf.php7](http://www.peacesoftware.de/einigewerte/calc_dampf.php7).
- Wolf, T. (2013). URL: <http://prjmgrcap.com/langfactorestimating.html>.
- Xu, D., Dong, L., and Ren, J. (2017). “Introduction of Hydrogen Routines”. In: *Hydrogen Economy*, pp. 35–54. DOI: [10.1016/b978-0-12-811132-1.00002-x](https://doi.org/10.1016/b978-0-12-811132-1.00002-x).
- Zeijden, P. T. van der (n.d.). *Industriewater in Nederland - VEMW*. URL: <https://www.vemw.nl/~media/VEMW/Downloads/Public/Water/Rapport%20Industriewater%20in%20Nederland.ashx>.





# MULTI CRITERIA ANALYSIS

In this appendix the multi criteria analyses of the hydrogen electrolysis and nitrogen purification

## **A.1. HYDROGEN ELECTROLYSIS**

The multi criteria analysis used to decide which hydrogen production method will be used.

### **A.1.1. PERFORMANCE CRITERIA**

The following performance criteria have been determined for the hydrogen production method.

1. The energy consumption should be minimized.
2. The CO<sub>2</sub> should be as low as possible.
3. The costs of the system should be as low as possible
4. The use of critical elements should be minimized
5. The system should be as small as possible
6. The lifetime of the system should be as long as possible

There is also one boundary condition; The hydrogen production system should have a technology readiness level of at least six. This is to ensure that the system is ready in the near future for large scale application.

### **A.1.2. WEIGHTINGS**

The criteria have been weighted to decide how important the criterion are.

	Energy consumption	CO2 emissions	Costs	Critical elements	Size	Lifetime	Integration Haber-Bosch	Total
Energy consumption		-	+	-	+	+	+	4
CO2 emissions	+		+	+	+	+	+	6
Costs	-	-		-	+	X	-	1
Critical elements	+	-	+		+	+	+	5
Size	-	-	-	-		-	-	0
Lifetime	-	-	X	-	+		-	1
Integration Haber-Bosch	-	-	+	-	+	+		3

Figure A.1: weightings of the hydrogen production criteria.

### A.1.3. CONCEPTS

All three hydrogen electrolysis methods will be used as a concept to be reviewed in the multi criteria analysis. From chapter 1, it is known that these methods are; alkaline electrolysis, polymer electrolyte membrane (PEM) electrolysis and solid oxide electrolysis.

Also being reviewed in the MCA is the production of hydrogen by biomass. All data considering biomass is also retrieved from chapter 1.

The last option for hydrogen production given in chapter 1. Was the thermochemical splitting of water using nuclear energy. However this option will be neglected, because of the political and financial challenges. Also the technology readiness level is 3-4, which does not meet the boundary condition of 6-7.

### A.1.4. MULTI CRITERIA ANALYSIS

The concepts are rated from one to five on each performance criteria.

	weight	Alkaline		PEM		Solid Oxide		Biomass	
		rate	score	rate	score	rate	score	rate	score
CO2 emissions	10	5	50	5	50	5	50	2	20
Critical elements	8	5	40	2	16	5	40	5	40
Energy consumption	7	3	21	3	21	5	35	4	28
Integration Haber-Bosch	6	3	18	3	18	1	6	1	6
Lifetime	4	5	20	3	12	1	4	4	16
Costs	4	5	20	3	12	1	4	2	8
Size	1	2	2	5	5	5	5	2	2
<b>Total</b>			<b>171</b>		<b>134</b>		<b>144</b>		<b>120</b>

Figure A.2: Multi criteria analysis of the hydrogen production.

## A.2. NITROGEN PURIFICATION

To decide which nitrogen purification method will be used a multi criteria analysis is performed.

### A.2.1. PERFORMANCE CRITERIA

The following performance criteria have been determined for the nitrogen purification process.

1. The energy consumption should be minimized
2. The costs should be as low as possible
3. The purity of the produced nitrogen should be as high as possible

### A.2.2. WEIGHTINGS

The criteria have been weighted to decide how important the criterion are.

	Energy consumption	Costs	Purity	Integration	Total
Energy consumption		+	+	+	3
Costs	-		-	-	0
Purity	-	+		+	2
Integration	-	+	-		1

Figure A.3: weightings of the nitrogen purification criteria.

### A.2.3. CONCEPTS

Three methods are considered for the nitrogen purification in chapter 1. The first is an air separation unit, also called cryogenic distillation. Where the air is cooled to very low temperatures so the different elements can be separated. The second option is pressure swing absorption. A special adsorbent material is used, which can adsorb the oxygen at specific pressure. Then the material can be separated from the air. The last method is membrane permeation, where a membrane is used. Only nitrogen can pass through the membrane.

### A.2.4. CRITERIA ANALYSIS

The concepts are rated from one to five on each performance criteria.

A

	weight	ASU		PSA		Membrane	
		rate	score	rate	score	rate	score
<b>Energy consumption</b>	10	5	<b>50</b>	4	<b>40</b>	3	<b>30</b>
<b>Purity</b>	8	5	<b>40</b>	4	<b>32</b>	3	<b>24</b>
<b>Integration</b>	7	1	<b>7</b>	2	<b>14</b>	3	<b>21</b>
<b>Costs</b>	4	5	<b>20</b>	4	<b>16</b>	2	<b>8</b>
<b>Total</b>			<b>117</b>		<b>102</b>		<b>83</b>

Figure A.4: multi criteria analysis of the nitrogen purification.

# B

ASPEN MODEL

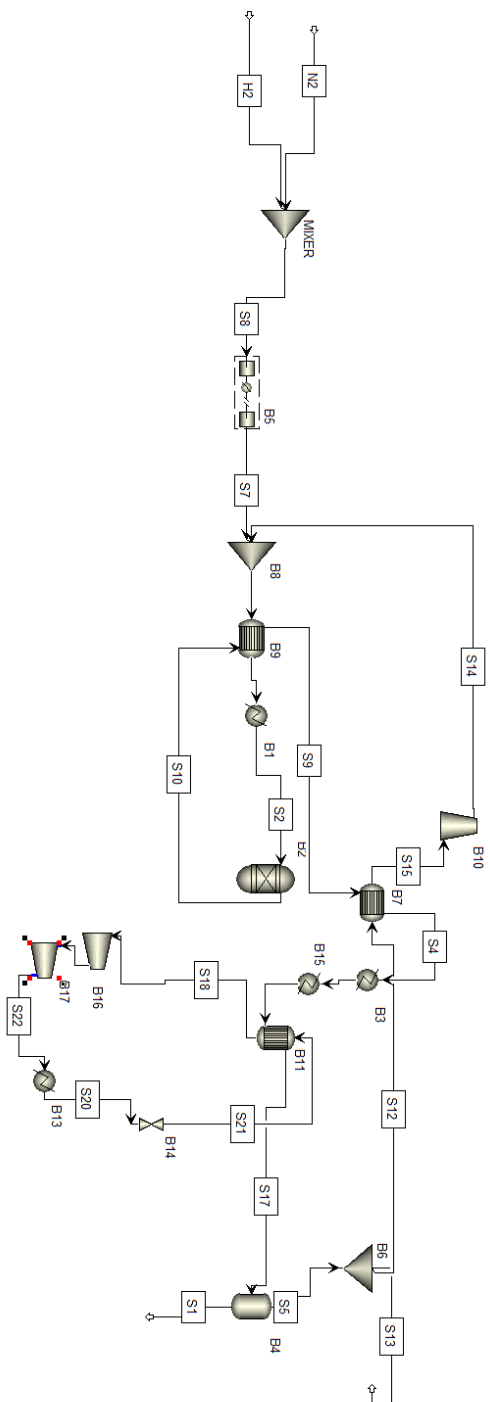


Figure B.1: Main flowsheet in Aspen containing relevant components and streams, excluding electrolysis and cryogenic distillation

# C

## PYTHON SCRIPTS HYDROGEN ELECTROLYSIS

### C.1. MASS BALANCE

```
1 #mass balance
2 m_h2 = 0.422 ** (24/6) #H2 flow rate in kg/s (variable)
3
4 n_h2 = m_h2/(2.01588/1000) #H2 flow rate in mol/s
5
6
7 v_h2o = 1          #stoichiometric number of H2O in electrolysis
8 reaction
9 v_o2 = 0.5        #stoichiometric number of O2 in electrolysis
10 reaction
11 v_el = 2          #number of electrons in electrolysis reaction
12
13
14 n_h2o = v_h2o * n_h2      #H2O flow rate in mol/s
15 n_o2 = v_o2 * n_h2       #O2 flow rate in mol/s
16
17 m_h2o = n_h2o * (18.01528/1000)    #H2O flow rate in kg/s
18 m_o2 = n_o2 * (31.998/1000)       #O2 flow rate in kg/s
19
20 m_inflow = m_h2o              #total inflow in kg/s
21 m_outflow = m_h2 + m_o2      #total outflow in kg/s
22
23 print('hydrogen flow rate:', m_h2, 'kg/s')
24 print('hydrogen flow rate:', n_h2, 'mol/s') #print('water flow rate
25 :', m_h2o, 'kg/s') print('water flow rate:', n_h2o, 'mol/s')
26 print('oxygen flow rate:', m_o2, 'kg/s')
27 print('oxygen flow rate:', n_o2, 'mol/s')
28 print('total inflow:', m_inflow, 'kg/s')
29 print('total outflow:', m_outflow, 'kg/s')
```

Listing C.1: Mass balance

```
In [1]: runfile('C:/Users/casvi/OneDrive/Documenten/WB jaar 3/ELECS/Q2/Python
electrolysis goed.py', wdir='C:/Users/casvi/OneDrive/Documenten/WB jaar 3/ELECS/
Q2')
hydrogen flow rate: 0.422 kg/s
hydrogen flow rate: 209.3378574121475 mol/s
water flow rate: 3.771280115879913 kg/s
water flow rate: 209.3378574121475 mol/s
oxygen flow rate: 3.349196380736948 kg/s
oxygen flow rate: 104.66892870607376 mol/s
total inflow: 3.771280115879913 kg/s
total outflow: 3.771196380736948 kg/s
```

Figure C.1: Results Python script mass balance

## C.2. ENERGY BALANCE

```
1 #energy balance
2 electricity_used = 237200 # electricity used to
split water in J/mol
3 heat_used = 48600 # heat used to split
water in J/mol
4 energy_used = electricity_used + heat_used # Energy used to split
water in J/mol
5 F = 96485 # Farradays number in C
/mol
6 E_0 = energy_used/ (v_el * F) # Thermoneutral voltage
in V
7 E_cell = 2 # cell voltage in V
8 total_energy_used = E_cell * v_el * F # total energy used for
electrolysis in J/mol
9 P_cell = total_energy_used * n_h2o # power of the
elctroloyzer in J/s = W
10
11 print('therom neutral voltage is:', E_0, 'V')
12 print('total energy used is:', total_energy_used, 'J/mol')
13 print('power of the cell:', P_cell, 'W')
14
15 #heat production
16 E_loss = E_cell - E_0 # overpotential converted into extra
heat in V
17 Q = E_loss * v_el * F # heat converted in J/mol
18 Q_cell = Q * n_h2 # heat converted in J/s or W
19
20 print('heat prodcuton:', Q, 'J/mol')
21 print('heat prodcuton:', Q_cell, 'W')
22
23 #efficiency
24 LHV = 285800 # higher heating value of
hydrogen in J/mol
25 HHV = 249200 # lower heating value of
hydrogen in J/mol
26 eff_HHV = HHV / total_energy_used # efficiency based on higher
heating value
27 eff_LHV = LHV / total_energy_used # efficiency based on lower
heating value
```

```

28 print('higher heating value efficiency:', eff_HHV)
29 print('lower heating value efficiency:', eff_LHV)
30
31
32 #yearly energy consumption and production
33 days_of_operation = 350
34     # days a year
35 hours_of_operation = 24
36     # hours a day
37 energy_consumption_1 = (P_cell * days_of_operation *
38     hours_of_operation)/1000 # yearly energy consumption in kWh
39 energy_consumption_2 = (energy_consumption_1 * 3600) / 1e12
40     # yearly energy consumption in PJ
41 hydrogen_production = m_h2 * 3600 *days_of_operation *
42     hours_of_operation # yearly hydrogen production in kg
43 print('yearly energy consumption:', energy_consumption_1, 'kWh')
44 print('yearly energy consumption:', energy_consumption_2, 'PJ')
45 print('yearly hydrogen production:', hydrogen_production, 'kg')
46
47 #cell area
48 i = 1000 # current denisty of the cell in A/m^2
49 I_cell = P_cell/E_cell # cell current in A
50 area_cell = I_cell/i # Area of cells needed in m^2
51 print('current density:', i, 'A/m^2')
52 print('current in the cell:', I_cell, 'A')
53 print('cell area needed:', area_cell, 'm^2')

```

C

Listing C.2: Energy balance

```

In [1]: runfile('C:/Users/casvi/OneDrive/Documenten/WB jaar 3/ELECS/Q2/Python
electrolysis goed.py', wdir='C:/Users/casvi/OneDrive/Documenten/WB jaar 3/ELECS/
Q2')
therom neutral voltage is: 1.481059232004975 V
total energy used is: 385940 J/mol
power of the cell: 80791852.68964422 W
heat prodction: 100139.99999999999 J/mol
heat prodction: 20963093.04125245 W
higher heating value efficiency: 0.6456962222107063
lower heating value efficiency: 0.7405296160024875
yearly energy consumption: 678651562.5930115 kWh
yearly energy consumption: 2.443145625334841 PJ
yearly hydrogen production: 12761280.0 kg
current density: 1000 A/m^2
current in the cell: 40395926.34482211 A
cell area needed: 40395.92634482211 m^2

```

Figure C.2: Results Python script energy balance



# D

## ENERGY CONSUMPTION

In this appendix the calculations for the energy consumption of the ammonia production process are given.

The assumptions made for the calculations are a production capacity around 8 ton ammonia per hour, 24 hours per day and 350 days per year. To reach a production capacity around 67,500 ton per year.

### D.1. AMMONIA SYNTHESIS

In this section the energy consumption of the ammonia synthesis loop is determined. The energy consumption is divided in compressors and heaters.

#### D.1.1. COMPRESSORS

the ammonia synthesis loop contains two compressors; a multi-stage compressor of 3176 kW and a recycle compressor of 84 kW. The multi-stage compressor will consume 26.68 GWh per year and the recycle compressor 0.71 GWh per year.

Also the refrigeration cycle, used to cool the product to  $-33\text{ }^{\circ}\text{C}$ , will need a compressor. This compressor has a power output of 718 kW. So the total consumption will be 6.03 GWh/y.

#### D.1.2. HEATERS

After the heat consumption and generation of different parts of the process are leveled, using pinch technology, some parts still needs additional heating. An impedance heater is needed to deliver a heat of 3006 kW. Because electrical heaters convert all the electricity into heat, the efficiency will be 100% (Energy.gov, n.d.). This means that also 3006 kW of electricity is used, resulting in 25.25 GWh per year.

## D.2. HYDROGEN ELECTROLYSIS

To reach the production capacity of 8 ton ammonia per hour, the production capacity of the hydrogen electrolysis needs to be 1.52 ton hydrogen per hour. When this production capacity is used in the python model it gives a energy consumption of 678.65 GWh per year.

## D.3. NITROGEN PURIFICATION

Although the cryogenic distillation, which is used to purify the ammonia, is not in the system boundaries. The energy consumption of this process will still be determined. This value is needed, in order to make a estimation for the  $CO_2$  emissions and costs. The energy consumption of cryogenic distillation is around 0.1 kWh/kg  $N_2$  (Rouwenhorst *et al.*, 2021). With a production capacity of 7.02 ton per hour. This results in a energy consumption of 5.91 GWh per year.

## D.4. COOLING AND REGENERATION

After the pitch technology is applied, some parts of the process still need extra cooling. This excess heat can be used to generate electricity using a steam turbine.

From appendix G can be used that the cooling of the reactor can regenerate 542 kW. This will result in 4.55 GWh per year of electricity generated.

## D.5. TOTAL

In table D.1 the total energy consumption is given.

Table D.1: Energy consumption of the renewable Haber-Bosch process per year.

	Power usage	Energy consumption
compressors	3,978 kW	33.42 GWh/y
heaters	3,006 kW	25.25 GWh/y
hydrogen electrolysis	80,792 kW	678.65 GWh/y
nitrogen purification	704 kW	5.91 GWh/y
total	87,939 kW	743.23 GWh/y

## D.6. WIND FARM FOR CASE TWO

The wind farm used will have a maximum rated power equal to the power consumption of the renewable process, so 88 MW (see table D.1). A wind farm on the north sea will have around 4,000 equivalent full-load hours (RVO, 2016), resulting in an energy production of 352 GWh per year.

This means the energy consumed from the grid will equal to 391.23 GWh per year in case two.

# E

## SIZING & SCALING

This section is meant to go further into detail regarding the sizing and scaling of key components.

### E.1. REACTOR SIZING

The reactor sizing follows the methodology of AIChE, 2019. The reactor is modeled as an axial flow reactor which are typically used in ammonia synthesis due to the low pressure drop throughout. The reactor feed flows through the catalyst tubes which then radially flow out of the reactor. The diameter of the reactor can be determined through eq. (E.1) and eq. (E.2).

$$D_s = d_{tube} \sqrt{\frac{n_{tube}}{\Phi}} \quad (E.1)$$

$$\Phi = \frac{\pi}{2\alpha^2\sqrt{3}} \quad (E.2)$$

Here  $D_s$  is the shell diameter,  $d_{tube}$  is the diameter of a tube,  $\Phi$  is the fraction of perforation,  $n_{tube}$  is the amount of catalyst tubes, and  $\alpha$  is the tube spacing coefficient, which means the space between the center of each tube is equal to  $\alpha \cdot d_{tube}$ . An Fe-based catalyst will be used, so the density of the catalyst is  $7874 \text{ kg/m}^3$  as given by Wikipedia, 2022. A tube diameter of 10 cm was chosen in line with previous literature (AIChE, 2019).

$$n_{tubes} = \frac{\pi d_{tube}^2 L_{tube}}{4} \rho_{cat} \quad (E.3)$$

The number of tubes required can be calculated with eq. (E.3), where  $L_{tube}$  is the length of the tube and  $\rho_{cat}$  is the density of the catalyst. A tube length of 6.5 m is chosen as this allows for maximum performance for the three bed reactor (Khademi and Sabbaghi, 2017). Where the first bed is 4 m, second bed is 1.5 m and third bed is 0.5 m (Burhan Kabir Suhan *et al.*, 2022).

$$n_{tubes} = \frac{\pi(0.10 \text{ m})^2(6 \text{ m})}{4} (7874 \frac{\text{kg}}{\text{m}^3}) = 495 \text{ tubes}$$

The tube spacing coefficient  $\alpha$  is chosen to be 1.5, to remain consistent with other literature. The fraction of perforation  $\Phi$  and the shell diameter are then calculated to be:

$$\Phi = \frac{\pi}{2(1.5)^2\sqrt{3}} = 0.403$$

$$D_s = (0.10 \text{ m})\sqrt{\frac{495}{0.403}} = 3.5 \text{ m}$$

The vessel is assumed to be a cylinder with hemispherical caps at both ends. Combining both caps gives a sphere with a diameter equal to  $D_s$ . So the total length of the reactor is:

$$L_{reactor} = L_{tube} + D_s \quad (\text{E.4})$$

$$L_{reactor} = 6\text{m} + 3.5\text{m} = 9.5\text{m}$$

The volume of the reactor can be determined using the same assumption of the cylindrical shape:

$$V_{reactor} = \frac{\pi D_s^2 L_{tube}}{4} + \frac{4\pi (\frac{D_s}{2})^3}{3} \quad (\text{E.5})$$

$$V_{reactor} = \frac{\pi(3.5 \text{ m})^2(6 \text{ m})}{4} + \frac{4\pi(1.75 \text{ m})^3}{3} = (57.7 \text{ m}^3) + (22.5 \text{ m}^3) = 80.2 \text{ m}^3$$

## E.2. FLASH SEPARATOR SIZING

The flash separator is modeled as a thin-walled vertical pressure vessel of cylindrical shape with hemispherical caps at both ends made of 304 stainless steel. Stainless steel is more expensive than carbon steel but has a higher corrosion resistance. The flash separator is designed to hold ammonia for 30 minutes with regards to safety standards (AIChE, 2019). The Aspen Plus simulation gives a volumetric flow entering the flash drum of 140.7 m<sup>3</sup>/h. The required volume of the flash drum can then be calculated with eq. (E.6).

$$V_{flash} = Q_{in} * \Delta t \quad (\text{E.6})$$

Where  $V_{flash}$  is the volume of the flash,  $Q_{in}$  is the volumetric flow entering the flash and  $\Delta t$  is the hold time. This gives a volume of:

$$V_{flash} = (140.7 \frac{\text{m}^3}{\text{h}}) (\frac{30 \text{ min}}{60 \text{ min/h}}) = 70.35 \text{ m}^3$$

Design parameters regarding diameter, wall thickness and safety factors are taken from Burhan Kabir Suhan *et al.*, 2022. The inside diameter of the pressure vessel is 3000 mm, wall thickness is 112 mm, head thickness is 62 mm and safety factor of 1.5. The head thickness is lower due to hemispherical shapes being able to withstand higher pressures than cylindrical shapes.

Considering the flash separator is modeled as a thin-walled cylinder with hemispherical caps, the volume can be written as:

$$V_{flash} = 2\pi r_{flash} L_{flash} + 4\pi r_{flash}^2 \quad (E.7)$$

Where  $r_{flash}$  is the radius of the vessel and  $L_{flash}$  is the length of the cylindrical part. Rewriting eq. (E.7) for  $L_{flash}$  and substituting parameters gives:

$$L_{flash} = \frac{V_{flash} - 4\pi r_{flash}^2}{2\pi r_{flash}} = \frac{(70.4m^3) - 4\pi(1.5m)^2}{2\pi(1.5m)} = 4.47m$$

Because the flash separator is thin walled, the mass is determined with eq. (E.8).

$$m_{flash} = (2\pi r_{flash} L_{flash} t_{wall} + 4\pi r_{flash}^2 t_{head}) * \rho_{steel} \quad (E.8)$$

Where  $t_{wall}$  is the wall thickness (112 mm),  $t_{head}$  is the head thickness (62 mm) and  $\rho_{steel}$  the density of 304 stainless steel (7930 kg/m<sup>3</sup>).

The mass of the flash drum is equal to:

$$m_{flash} = (2\pi(1.5m)(4.47m) * (0.112m) + 4\pi(1.5m)^2(0.062m)) * 7930 = 41842kg$$

### E.3. NITROGEN PRESSURE VESSEL

Considering the fact that this process will produce nitrogen during off peak hours when electricity is cheaper and not needed for households, there is a need for nitrogen storage. The required storage volume of nitrogen is 220,000 L as discussed in section 2.2.2. To make a cost estimation of the pressure tank an evaluation of the shell mass is to be made. The pressure tank is modelled as a thin-walled vertical pressure vessel of cylindrical shape with hemispherical caps at both ends made of 304 stainless steel. The diameter of this tank is equal to 3 m and the wall thickness is 100 mm, comparable to the vessels manufactured by Cryolor, 2019.

The volume of the tank is described by eq. (E.9). Where  $V_{tot}$  is the total volume of the tank,  $r$  is the radius of the tank and  $L_{cylinder}$  is the length of the cylindrical part of the tank.

$$V_{tot} = \pi r^2 L_{cylinder} + \frac{4}{3} \pi r^3 \quad (E.9)$$

Rewriting for  $L_{cylinder}$  gives:

$$L_{cylinder} = \frac{V_{tot} - \frac{4}{3} \pi r^3}{\pi r^2} = \frac{(222m^3) - \frac{4}{3} \pi (1.5m)^3}{\pi (1.5m)^2} = 29.4 m$$

The mass is determined by eq. (E.10). Where  $m_{shell}$  is the mass of the shell and  $t_{wall}$  is the wall thickness (100 mm) and  $\rho_{ss}$  is the density of 304 stainless steel (7930 kg/m<sup>3</sup>).

$$m_{shell} = (2\pi r * l_{cylinder} + 4\pi r^2) t_{wall} \rho_{ss} \quad (E.10)$$

Solving this equation gives:

$$m_{\text{shell}} = (2\pi(1.5 \text{ m})(29.4 \text{ m}) + 4\pi(1.5 \text{ m})^2)(0.1 \text{ m})(7930 \text{ kg/m}^3) = 241,865 \text{ kg}$$

#### E.4. HYDROGEN STORAGE VESSEL

The possibility to store hydrogen gives the ability to produce the hydrogen during off peak hours. The hydrogen rate requirement is equal to 1.52 ton  $H_2$  per hour, which is 36.5 ton  $H_2$  per day.

Table E.1: Data on hydrogen storage with the storage pressure, the corresponding hydrogen density and maximum storage vessel size and the storage space and tanks needed with 36.5 ton  $H_2$  per day. Data from (RoadstoHy2, 2013)

pressure	density	storage volume	maximum tank size	number of tanks
700 bar	0.042 $\text{tonH}_2/\text{m}^3$	869 $\text{m}^3$	0.2 $\text{m}^3$	4345 tanks
300 bar	0.020 $\text{tonH}_2/\text{m}^3$	1825 $\text{m}^3$	1 $\text{m}^3$	1825 tanks
10 bar	8.085E-4 $\text{tonH}_2/\text{m}^3$	45,145 $\text{m}^3$	15000 $\text{m}^3$	3 tanks

# F

## TECHNO-ECONOMIC ANALYSIS

<b>Opex (2030)</b>				
<b>Fixed Capital (Capex)</b>	241377854,1			
<b>Raw materials/ Utilities</b>	Industry water	Electricity		Total
<b>Price (€/m3 and €/kWh)</b>		0,457	0,0758	
<b>Total use (m3 and kWh)</b>	2058000		7,43E+08	
<b>Total Price (€)</b>	940506		5,63E+07	57259906
<b>Operating labour</b>	6495958			
<b>Miscellaneous materials</b>	1810333,906			
<b>Maintenance</b>	18103339,06			
<b>Laboratory costs</b>	1396630,97			
<b>Supervision</b>	1299191,6			
<b>Plant overheads</b>	3247979			
<b>Capital charges</b>	24137785,41			
<b>Insurance</b>	24137785,41			
<b>Royalties</b>	24137785,41			
<b>Direct production costs</b>	162026694,8			
<b>Sales expenses</b>	40506673,69			
<b>Total operational costs</b>	202533368,5			
<b>Annual production (kg)</b>	67200000			
<b>Sales price/kg NH3</b>	1,16			
<b>Annual Sales</b>	77952000			
<b>Net profit</b>	-93436026,35			
<b>Cash flow</b>	-124581368,5			

Figure F.1: Operation costs with an electricity price of 0,0758 €/kWh and a sales price of 1,315€/kg NH<sub>3</sub>

	Year	Cash flow	Denominator (1+i) <sup>n</sup>	Present value	Net present value
Construction - Begins 2027	1	-81947781,48	1,08	-€ 75.877.575,44	-€ 75.877.575,44
	2	-83463815,43	1,1664	-€ 71.556.769,06	-€ 147.434.344,50
	3	-85007896,02	1,259712	-€ 67.482.008,60	-€ 214.916.353,11
Operation - Begins 2030	4	-124581368,5	1,36048896	-€ 91.571.024,93	-€ 306.487.378,03
	5	-126886123,8	1,469328077	-€ 86.356.563,78	-€ 392.843.941,82
	6	-153082128,4	1,586874323	-€ 96.467.707,76	-€ 489.311.649,58
	7	-169691539,4	1,713824269	-€ 99.013.383,38	-€ 588.325.032,96
	8	-188103071,4	1,85093021	-€ 101.626.236,56	-€ 689.951.269,52
	9	-208512254,6	1,999004627	-€ 104.308.040,02	-€ 794.259.309,54
	10	-231135834,3	2,158924997	-€ 107.060.613,30	-€ 901.319.922,84
	11	-256214072,3	2,331638997	-€ 109.885.823,93	-€ 1.011.205.746,77
	12	-284013299,1	2,518170117	-€ 112.785.588,73	-€ 1.123.991.335,49
	13	-314828742,1	2,719623726	-€ 115.761.875,10	-€ 1.239.753.210,59
	14	-348987660,6	2,937193624	-€ 118.816.702,35	-€ 1.358.569.912,94
	15	-386852821,8	3,172169114	-€ 121.952.143,11	-€ 1.480.522.056,06
	16	-428826353	3,425942643	-€ 125.170.324,67	-€ 1.605.692.380,72
	17	-475354012,2	3,700018055	-€ 128.473.430,46	-€ 1.734.165.811,18
	18	-526929922,6	3,996019499	-€ 131.863.701,54	-€ 1.866.029.512,71
	19	-584101819,2	4,315701059	-€ 135.343.438,11	-€ 2.001.372.950,82
	20	-647476866,6	4,660957144	-€ 138.915.001,06	-€ 2.140.287.951,87
	21	-717728106,6	5,033833715	-€ 142.580.813,58	-€ 2.282.868.765,46
	22	-795601606,1	5,436540413	-€ 146.343.362,83	-€ 2.429.212.128,29
	23	-881924380,4	5,871463646	-€ 150.205.201,57	-€ 2.579.417.329,86
	24	-977613175,7	6,341180737	-€ 154.168.949,95	-€ 2.733.586.279,81
	25	-1083684205	6,848475196	-€ 158.237.297,24	-€ 2.891.823.577,04
	26	-1201263942	7,396353212	-€ 162.413.003,69	-€ 3.054.236.580,73
	27	-1331601079	7,988061469	-€ 166.698.902,40	-€ 3.220.935.483,13
	28	-1476079796	8,627106386	-€ 171.097.901,21	-€ 3.392.033.384,35

Figure E.2: Net Present Value (NPV) with an electricity price of 0,0758 €/kWh and a sales price of 1,315€/kg NH<sub>3</sub>

F

	Year	Cash flow	Denominator (1+i) <sup>n</sup>	Present value	Net present value
Construction - Begins 2027	1	-81947781,48	1,08	-€ 75.877.575,44	-€ 75.877.575,44
	2	-83463815,43	1,1664	-€ 71.556.769,06	-€ 147.434.344,50
	3	-85007896,02	1,259712	-€ 67.482.008,60	-€ 214.916.353,11
Operation - Begins 2030	4	9146631,532	1,36048896	€ 6.723.047,23	-€ 208.193.305,88
	5	9315844,215	1,469328077	€ 6.340.207,04	-€ 201.853.098,84
	6	11239127,01	1,586874323	€ 7.082.556,47	-€ 194.770.542,37
	7	12458572,29	1,713824269	€ 7.269.457,27	-€ 187.501.085,10
	8	13810327,38	1,85093021	€ 7.461.290,17	-€ 180.039.794,93
	9	15308747,9	1,999004627	€ 7.658.185,33	-€ 172.381.609,60
	10	16969747,05	2,158924997	€ 7.860.276,33	-€ 164.521.333,28
	11	18810964,6	2,331638997	€ 8.067.700,29	-€ 156.453.632,99
	12	20851954,26	2,518170117	€ 8.280.597,93	-€ 148.173.035,06
	13	23114391,3	2,719623726	€ 8.499.113,71	-€ 139.673.921,35
	14	25622302,76	2,937193624	€ 8.723.395,88	-€ 130.950.525,47
	15	28402322,61	3,172169114	€ 8.953.596,60	-€ 121.996.928,87
	16	31483974,61	3,425942643	€ 9.189.872,07	-€ 112.807.056,80
	17	34899985,85	3,700018055	€ 9.432.382,58	-€ 103.374.674,21
	18	38686634,32	3,996019499	€ 9.681.292,68	-€ 93.693.381,54
	19	42884134,14	4,315701059	€ 9.936.771,23	-€ 83.756.610,30
	20	47537062,7	4,660957144	€ 10.198.991,59	-€ 73.557.618,72
	21	52694834	5,033833715	€ 10.468.131,64	-€ 63.089.487,07
	22	5841223,49	5,436540413	€ 10.744.374,01	-€ 52.345.113,07
	23	64749949,74	5,871463646	€ 11.027.906,10	-€ 41.317.206,97
	24	71775319,28	6,341180737	€ 11.318.920,29	-€ 29.998.286,69
	25	79562941,42	6,848475196	€ 11.617.614,02	-€ 18.380.672,67
	26	88195520,57	7,396353212	€ 11.924.189,94	-€ 6.456.482,73
	27	97764734,55	7,988061469	€ 12.238.856,06	€ 5.782.373,34
	28	108372208,2	8,627106386	€ 12.561.825,88	€ 18.344.199,21

Figure E.3: Net Present Value (NPV) with an electricity price of 0,0758 €/kWh and a sales price of 3,15€/kg NH<sub>3</sub>

	Year	Cash flow	Denominator (1+i) <sup>n</sup>	Present value	Net present value
Construction - Begins	2027	1 -81947781,48	1,08	-€ 75.877.575,44	-€ 75.877.575,44
	2028	2 -83463815,43	1,1664	-€ 71.556.769,06	-€ 147.434.344,50
	2029	3 -85007896,02	1,259712	-€ 67.482.008,60	-€ 214.916.353,11
Operation - Begins	2030	4 12647131,53	1,36048896	€ 9.296.019,23	-€ 205.620.333,88
	2031	5 12881103,46	1,469328077	€ 8.766.662,58	-€ 196.853.671,30
	2032	6 15540444,27	1,586874323	€ 9.793.115,97	-€ 187.060.555,33
	2033	7 17226582,47	1,713824269	€ 10.051.545,42	-€ 177.009.009,92
	2034	8 19095666,67	1,85093021	€ 10.316.794,53	-€ 166.692.215,39
	2035	9 21167546,5	1,999004627	€ 10.589.043,27	-€ 156.103.172,11
	2036	10 23464225,3	2,158924997	€ 10.868.476,36	-€ 145.234.695,75
	2037	11 26010093,74	2,331638997	€ 11.155.283,38	-€ 134.079.412,38
	2038	12 28832188,91	2,518170117	€ 11.449.658,91	-€ 122.629.753,47
	2039	13 31960481,41	2,719623726	€ 11.751.802,69	-€ 110.877.950,78
	2040	14 35428193,65	2,937193624	€ 12.061.919,70	-€ 98.816.031,08
	2041	15 39272152,66	3,172169114	€ 12.380.220,36	-€ 86.435.810,72
	2042	16 43533181,22	3,425942643	€ 12.706.920,62	-€ 73.728.890,10
	2043	17 48256531,38	3,700018055	€ 13.042.242,14	-€ 60.686.647,96
	2044	18 53492365,04	3,996019499	€ 13.386.412,42	-€ 47.300.235,55
	2045	19 59296286,64	4,315701059	€ 13.739.664,97	-€ 33.560.570,58
	2046	20 65729933,74	4,660957144	€ 14.102.239,46	-€ 19.458.331,12
	2047	21 72861631,55	5,033833715	€ 14.474.381,89	-€ 4.983.949,24
	2048	22 80767118,58	5,436540413	€ 14.856.344,74	€ 9.872.395,51
	2049	23 89530350,94	5,871463646	€ 15.248.387,17	€ 25.120.782,68
	2050	24 99244394,02	6,341180737	€ 15.650.775,17	€ 40.771.557,85
	2051	25 110012410,8	6,848475196	€ 16.063.781,74	€ 56.835.339,58
	2052	26 121948757,3	7,396353212	€ 16.487.687,09	€ 73.323.026,67
	2053	27 135180197,5	7,988061469	€ 16.922.778,83	€ 90.245.805,50
	2054	28 149847248,9	8,627106386	€ 17.369.352,16	€ 107.615.157,66

Figure F.4: Net Present Value (NPV) with an electricity price of 0,025 €/kWh and a sales price of 2,50€/kg NH<sub>3</sub>



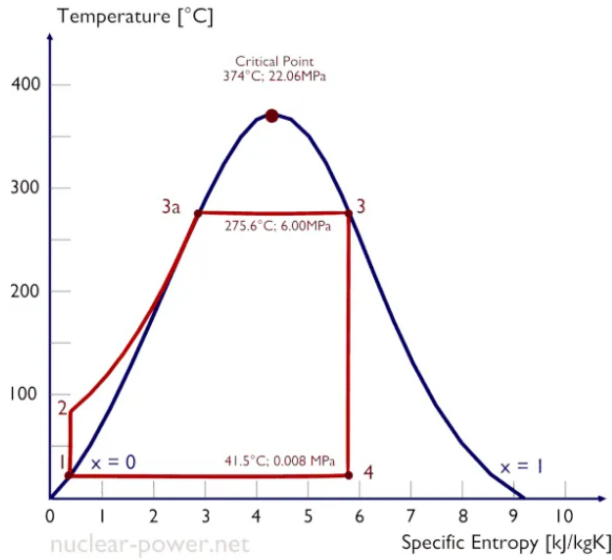
# G

## COOLING

Some parts of the ammonia production process produce excess heat. So these parts need extra cooling. The heat can be used to generate electricity using a steam turbine. In appendix [G.1](#), a calculation is made on how much electricity could be generated using this method.

### **G.1. POWER CYCLE**

A Rankine cycle is used to generate the electricity. Typical values for the boiler and condenser pressures are 60 bar and 0.08 bar respectively (*Boiler and condenser pressures - rankine cycle 2021*). Fig [G.1](#) gives a representation of a typical Rankine cycle.



nuclear-power.net

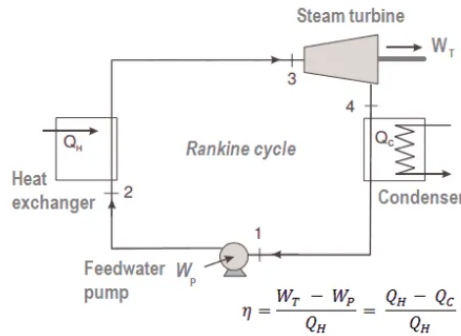


Figure G.1: Temperature vs entropy diagram and a schematic drawing of a Rankine cycle, taken from *Rankine cycle - steam turbine cycle: Characteristics 2021*

For this Rankine cycle the equations G.1 apply (Moran and Shapiro, 2010). With  $\dot{Q}_H$  the heat added to the boiler,  $\dot{W}_T$  the work done by the turbine,  $\dot{Q}_C$  the heat lost in the condenser,  $\dot{W}_P$  the work done by the pump and  $\dot{m}$  the mass flow of the cycle.

$$\begin{aligned}
 \text{Boiler: } \dot{Q}_H &= \dot{m}(h_3 - h_2) \\
 \text{Turbine: } \dot{W}_T &= \dot{m}(h_3 - h_4) \\
 \text{Condenser: } \dot{Q}_C &= \dot{m}(h_4 - h_1) \\
 \text{Pump: } \dot{W}_P &= \dot{m}(h_2 - h_1)
 \end{aligned}
 \tag{G.1}$$

Because of the low specific volume of a liquid the work provided by the pump ( $\dot{W}_P$ ) can be neglected (Muller-Steinhagen, 2011). Therefore equations G.1 can be rewritten as equations G.2.

$$\begin{aligned}
 h_1 &= h_2 \\
 \text{Boiler: } \dot{Q}_H &= \dot{m}(h_3 - h_1) \\
 \text{Turbine: } \dot{W}_t &= \dot{m}(h_3 - h_4) \\
 \text{Condenser: } \dot{Q}_c &= \dot{m}(h_4 - h_1) \\
 \text{Pump: } \dot{W}_p &= 0
 \end{aligned}
 \tag{G.2}$$

## G.2. REACTOR COOLING

The reactor in the ammonia synthesis loop needs cooling of 7200 kW, so  $\dot{Q}_H = 7200 \text{ kW}$ . The values of the specific enthalpy of the power cycle are given in table G.1 (Wischnewski, n.d.).

	Pressure	Temperature	State	Enthalpy
$h_1$	0.08 bar	41.5 C	liquid	174 kJ/kg
$h_3$	60 bar	275.6 C	gas	2785 kJ/kg
$h_4$	0.08 bar	41.5 C	gas	2576 kJ/kg

Table G.1: specific enthalpy at the different stages of the power cycle, enthalpy values from Wischnewski, n.d.

With these values the mass flow is equal to 2.76 kg/s, see equation G.3.

$$\dot{m} = \frac{\dot{Q}_H}{h_3 - h_1} = \frac{7200 \text{ kW}}{(2576 - 174) \text{ kJ/kg}} = 2.76 \text{ kg/s}
 \tag{G.3}$$

Therefore the heat flow and work of the power cycle follow:

$$\text{Boiler: } \dot{Q}_H = 7,200 \text{ kW}
 \tag{G.4}$$

$$\text{Turbine: } \dot{W}_T = 577 \text{ kW}
 \tag{G.5}$$

$$\text{Condenser: } \dot{Q}_C = 6,630 \text{ kW}
 \tag{G.6}$$

$$\text{Pump: } \dot{W}_P = 0 \text{ kW}
 \tag{G.7}$$

The steam turbine delivers 577 kW of work. With a generator efficiency of 94%, this means that 542 kW of electricity is produced (EPA, 2015).

## G.3. ECONOMIC FEASIBILITY

The installed costs<sup>1</sup> of a turbine are 1,005 €/kW (DoE, 2016). So a 542 kW will have total cost around €545,000. While the operating cost are 0.0088 €/kWh and the yield of the turbine is 0.09 €/kWh. So the net yield per year is equal to €370,000. For 25 years it means the yield is €9.25 million. Thus the inclusion of the turbine is economic feasible.

<sup>1</sup>The euro-dollar exchange rate used is 1€ = 1.13\$